AFFIDAVIT

I declare that I have authored this thesis independently, that I have not used other than the declared sources/resources, and that I have explicitly indicated all material which has been quoted either literally or by content from the sources used. The text document uploaded to TUGRAZonline is identical to the present master‘s thesis dissertation.

Date

Signature

Acknowledgements

First of all, I would like to thank Karl Gruber for supervising this master thesis. He recommended to work on this project and gave some great advice regarding structure refinement, presentation techniques and job applications. He was always available and willing to help in case there would be any questions.

I am very thankful to Prashant Kumar. He was a great teacher and I learned a lot from him. Also, he was very enthusiastic about the project and very motivating. Of course I also want to thank Manuel Reisinger, who worked a lot on the DPP III project and was a great help during the writing process.

I also would like to thank Tea Pavkov-Keller for her advice and Silvia Wallner for help with the ITC experiments. And of course I want to thank the whole Strubi-group for providing a nice working environment.

Last but not least, I am very grateful to my family for their support during my master's course.

Abstract

Dipeptidyl peptidase III (DPP III) is a Zn-dependent aminopeptidase, cleaving dipeptides from the N-terminal end of a broad variety of oligopeptides. The monomeric protein consists of 737 amino acids and is proposed to be involved in pain modulatory system and protein turnover. Moreover, it was found to be overexpressed in certain types of cancer and it is a member of the human central proteome. To understand how DPP III is able to bind the wide variety of substrates it seems to accept, crystallographic studies were performed. Another aim of the thesis was to confirm the proposed catalytic mechanism of human DPP III and confirm the suspected formation of an anion-π interaction important for catalysis. The structure of human DPP III was determined in complex with met-enkephalin and endomorphin-2. Structures determined in this thesis and structures of inactive hDPP III in complex with other ligands (angiotensin-II, leu-enkephalin and IVYPW) were analyzed. The ligands were found to bind to the 5-stranded β-core of the protein and a different binding mode was observed for ligands acting as substrates and those acting as inhibitors. The proposed catalytic mechanism (water-mediated catalysis) was confirmed, as well as the suspected anion-π interaction between Phe-373 and Glu-451.

Zusammenfassung

Dipeptidyl peptidase III (DPP III) ist eine Zn-abhängige Aminopeptidase, die zwei Aminosäuren vom N-terminalen Ende unterschiedlicher Oligopeptiden spaltet. Es handelt sich um ein 737 Aminosäuren großes Monomer, das wahrscheinlich in Schmerzwahrnehmung und Proteinumsatz involviert ist. Humane DPP III ist in bestimmten Krebsarten überexprimiert und ist Teil des human central proteome. In der vorliegenden Masterarbeit soll untersucht werden, wie DPP III die Vielfalt an Substraten bindet, die es umzusetzen scheint. Außerdem sollen der katalytische Mechanismus und eine vermutete Anionen-π Interaktion bestätigt werden. Die Struktur von humaner DPP III wurde im Komplex mit Met-Enkephalin und im Komplex mit Endomorphin-2 bestimmt. Des weiteren wurden Strukturen, die in dieser Arbeit bestimmt wurden, und Strukturen im Komplex mit anderen Liganden (Angiotensin-II, Leu-Enkephalin und IVYPW) analysiert. Die analysierten Liganden binden am 5-strängigen β-Faltblatt, das den Kern der unteren Domäne des Proteins bildet. Ein unterschiedlicher Bindemodus für Substrate und Liganden, die nur sehr langsam hydrolysiert werden, wurde beobachtet. Der vorgeschlagene katalytische Mechanismus (Wasser-vermittelte Katalyse) und die vermutete Anionen-π Interaktion zwischen Phe-373 und Glu-451 konnten bestätigt werden.

Table of contents

Affidavit....2

Acknowledgements....3

Abstract....4

Zusammenfassung....5

1. INTRODUCTION 8

2. MATERIALS AND METHODS 14

2.1 Cloning and site-directed mutagenesis....14

2.2 Protein expression and purification....16

2.3 Protein crystallization trials....18

2.4 Protein structure determination....19

2.5 Fluorescent activity assay....20

2.6 Isothermal titration calorimetry (ITC)....20

3. RESULTS 22

3.1 Site-directed mutagenesis....22

3.2 Protein purification....23

3.3 Protein structure determination....27

3. 3. 1 hDPP III in complex with met-enkephalin....30

3. 3. 2 hDPP III in complex with endomorphin-2....32

3.4 Fluorescent activity assay....35

3.5 Isothermal titration calorimetry (ITC)....36

4. DISCUSSION **37**

4.1 Structures of hDPP III in complex with various ligands.....37

4. 1. 1 hDPP III in complex with tynorphin.....39

4. 1. 2 hDPP III in complex with angiotensin-II.....40

4. 1. 3 hDPP III in complex with leu-enkephalin.....42

4. 1. 4 hDPP III in complex with IVYPW.....43

4.2 Binding modes and their influence on catalysis.....44

4.3 Anion-π interaction.....47

4.4 Conclusions.....49

5. LIST OF FIGURES **50**

6. LIST OF TABLES **52**

7. REFERENCES **53**

8. APPENDIX **56**

1. Introduction

Dipeptidyl peptidase III (DPP III), also referred to as enkephalinase B, is a Zn-dependent aminopeptidase, sequentially cleaving dipeptides from the N-terminal end of a broad variety of oligopeptides [1].

DPP III in solution is a monomeric protein. Due to its unique catalytic motif (HEXXGH), DPP III was assigned to the M49 family of metallopeptidases and so far represents the only member of this family. Glu in the HEXXGH motif is crucial for substrate hydrolysis, both His are involved in Zn-ion coordination. A third residue coordinating the Zn-ion is a Glu, which is part of another conserved motif, the secondary motif EEXRAE/D [1]. A water molecule was observed to be in contact with the Zn-ion and is proposed to be important for catalysis [2, 3]. Tetraeptides to decapeptides with strong diversity regarding their amino acid composition and sequence were shown to be cleaved by DPP III [1].

DPP III was identified in a variety of procaryotic and eucaryotic organisms and is therefore considered a ubiquitous protein. The peptidase is located in the cytosol, although membranous forms of DPP III have been reported [1]. Human dipeptidyl peptidase III (hDPP III) was identified as part of the human central proteome [4].

The enzyme is proposed to be involved in several physiological mechanisms, its exact roles are still unclear.

Implication of DPP III in pain modulatory system has been suggested based on several findings [1]. hDPP III was found in cerebrospinal fluid of individuals suffering from acute pain [5] and rat DPP III was localized in the superficial laminae of the dorsal horn, which contains a high concentration of enkephalins [6]. Enkephalins are opioid peptides with pain killing or opiate activity, to which DPP III shows a high in vitro affinity [1, 6]. Furthermore, DPP III shows a high in vitro affinity to endomorphins in, another class of opioid peptides [1].

DPP III also hydrolyzes angiotensins (angiotensin II, III and IV), which are the main peptide contributors of the renin-angiotensin system [1, 7]. This suggests DPP III is involved in blood pressure regulation [1].

A contribution of DPP III to the cytosolic protein turnover is proposed [1]. Its post-proline activity enables DPP III to degrade peptides that are otherwise resistant to most aminopeptidases involved in protein turnover [1, 8].

DPP III was found to be overexpressed in certain types of cancer. An increase of DPP III activity was measured in endometrial and ovarian malignant tumors [9, 10], enhancement of its activity in ovarian primary carcinoma was observed to be directly correlated to the aggressiveness of the tumor [10]. Furthermore, involvement of DPP III in cataractogenesis and defense against oxidative stress has been described [11, 12].

Several structures of DPP III were determined, among them one structure of yeast DPP III (yDPP III) [2] and three structures of hDPP III [3].

Structures of yDPP III (PDB: 3CSK) and hDPP III without ligand (PDB: 3FVY) are shown in figure 1. DPP III is an elongated protein, consisting of two domains. The upper domain mostly consists of α-helices and carries the HEXXGH and EEXRAE/D motif. The lower domain consists of α-helices and β-sheets mixed. It contains the 5-stranded β-core, which is proposed to be involved in ligand binding. The domains are separated by a wide cleft, in which the substrate binding site is located and connected by a helical loop originating from the lower domain. His-460, His-465 (from 460-HEXXGH-465) and Glu-517 (from 516-EEXRAE/D-521) coordinate the Zn-ion in yDPP III. His-450, His-455 (from 450-HEXXGH-455) and Glu-508 (from 507-EEXRAE/D-512) coordinate the Zn-ion in hDPP III. In both structures, a water molecule was observed bound to the Zn-ion. Glu-461 in yDPP III or Glu-451 in hDPP III has been suggested to play a crucial role in the catalytic mechanism [2, 3]. Exchange of this residue with Ala abolishes enzyme activity [13].

Water-mediated cleavage of the scissile peptide bond, similar to the catalytic mechanisms of other metallopeptidases like thermolysin and neprolysin, has been proposed to be the catalytic mechanism of DPP III. Glu-461 (yDPP III), acting as a general base, deprotonates the water molecule in contact with the Zn-ion, which thereby becomes a nucleophile. The nucleophile attacks the carbonyl carbon of the scissile peptide bond. Glu-461, now acting as a general acid, provides a proton to the leaving nitrogen group. This leads to breakage of the peptide bond. Another conserved residue proposed to be involved in the

catalytic mechanism is His-578 in yDPP III or His-568 in hDPP III, which is proposed to stabilize the oxyanion intermediate [2, 3].

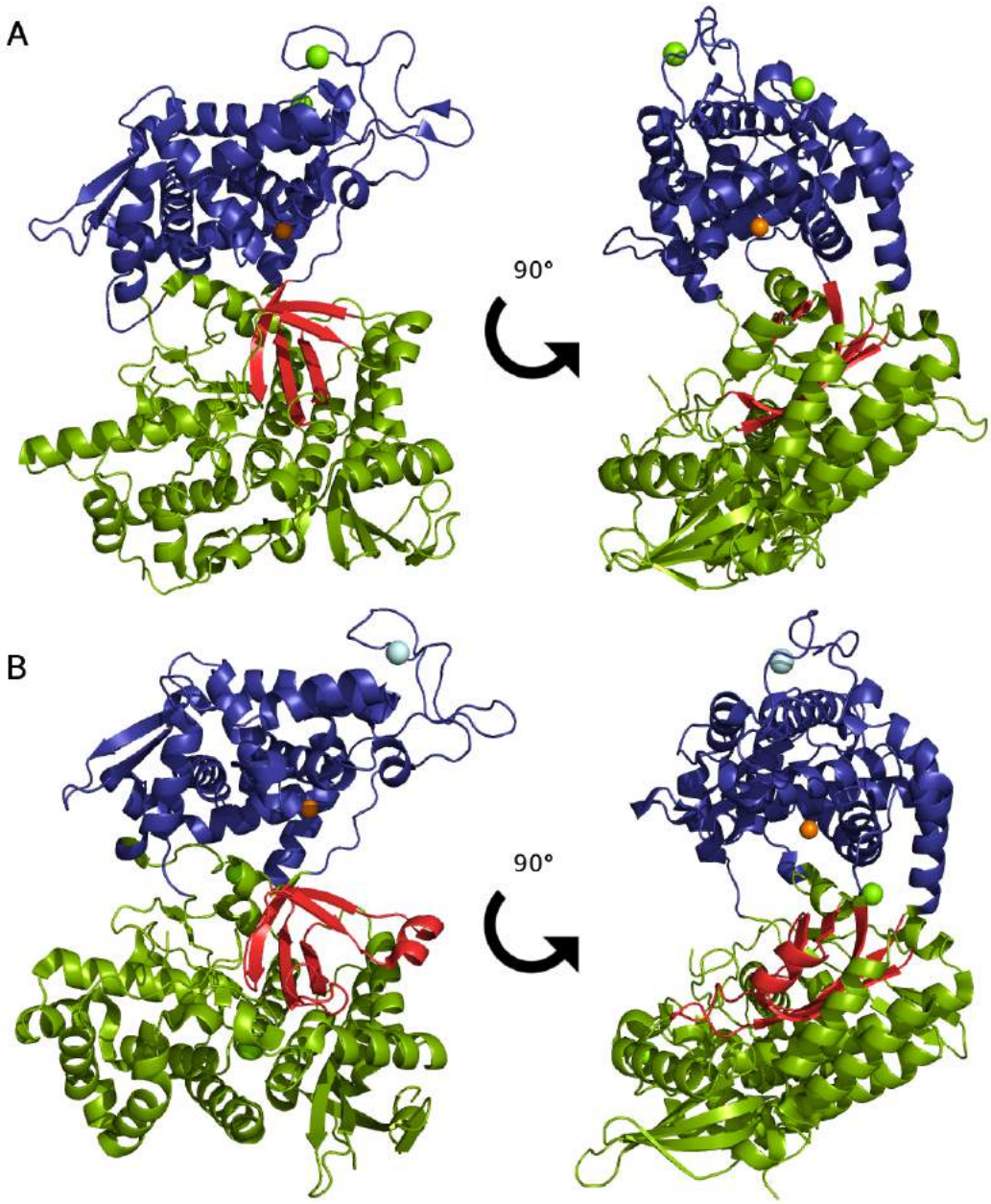

Figure 1: Open yDPP III and hDPP III

A: Structure of yDPP III without ligand bound in two different orientations. The upper lobe is shown in blue, the lower lobe is shown in green, the 5-stranded β-core is colored red. The structure contains a Zn-ion (orange) and two Mg-ions (green spheres). **B**: Structure of hDPP III without ligand. The upper lobe is colored blue, the lower lobe is shown in green, the 5-stranded β-core in red. The structure contains a Zn-ion (orange), two Mg-ions (green spheres) and a Cl-ion (light blue).

The structure of hDPP III in complex with tynorphin (VVYPW), a synthetic peptide that was shown to be a potent inhibitor of DPP III [14], is pictured in figure 2 (PDB: 3T6B). Tynorphin-bound hDPP III was observed to have an almost globular shape. It is suggested that, upon substrate binding, a large entropy-driven domain movement occurs. The amino acids 409 – 420 work as a „mechanical hinge", upper and lower domain move towards each other as rigid bodies. The 5-stranded β-core of hDPP III was found to be involved in tynorphin binding [3].

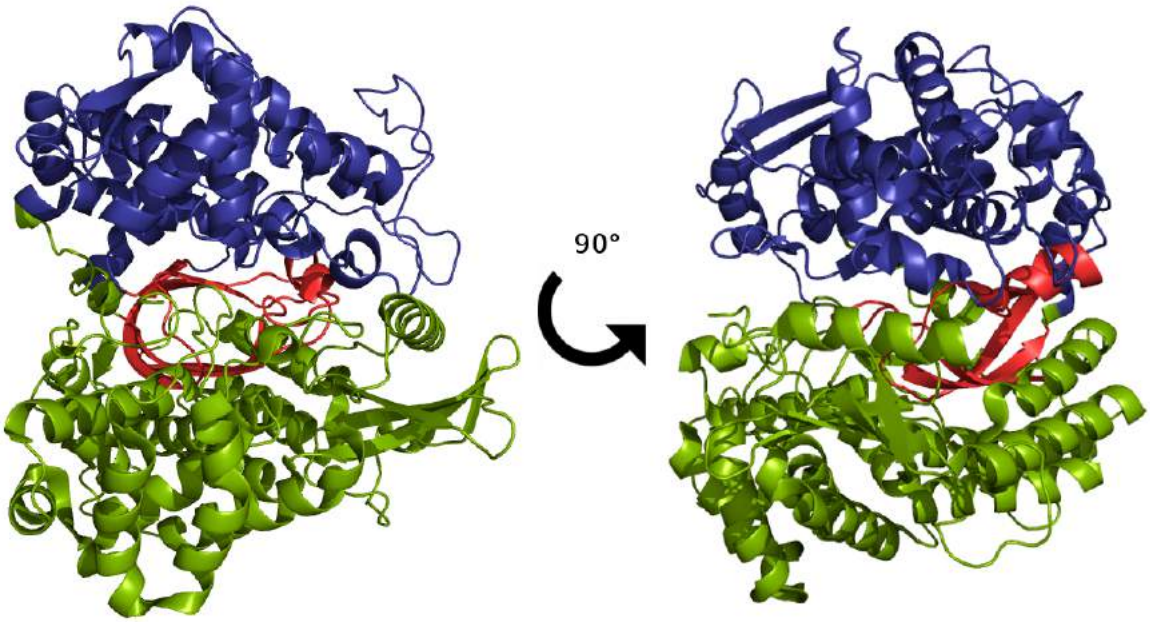

Figure 2: hDPP III in complex with tynorphin

The structure of closed hDPP III is shown in two different orientations, tynorphin is not pictured in the binding cleft. The upper lobe is colored blue, the lower lobe is shown in green and the 5-stranded β-core is colored red.

Although a structure of DPP III in complex with a ligand has already been determined [3], it is still unclear how the protein is able to adapt to the wide variety of ligands it seems to accept and if binding of other peptides induces the same domain motion. Aim of this thesis is to investigate this subject by crystallizing hDPP III in complex with ligands of various length and amino acid composition. The endogenous opioid peptides valorphin (VVYPWTQ), met-enkephalin (YGGFM) and endomorphin-2 (YPFF-NH_2) were used for

cocrystallization [1, 6, 15], as well as angiotensin-II (DRVYIHPF), a peptide involved in blood vessel constriction [1, 7]. As there is no information about the thermodynamic properties of angiotensin-II and hDPP III available, Isothermal Titration Calorimetry (ITC) was performed. Furthermore, Arg-Arg-β-naphthylamide (AaβNA) was used for cocrystallization, a synthethic ligand that was shown to be a good substrate of hDPP III [16].

Another aim of this thesis is to gain more information about the catalytic mechanism, which was achieved by determination of the structure of hDPP III in complex with different ligands too.

In order to confirm the presence of an anion-π interaction playing a role in putting the catalytic Glu-451 in place, fluorescent activity assays were carried out. Positioning of the catalytic residue via an anion-π interaction has been described in ketosteroid isomerase active site, in which a Phe interacts with the catalytic Asp [17].

The thesis is part of a project, in which hDPP III was also crystallized in complex with the opioid peptide leu-enkephalin [1] and in complex with the synthetic inhibitor IVYPW [6]. Crystallization and structure determination of hDPP III and leu-enkephalin were done by Prashant Kumar, as well as structure determination of hDPP III in complex with angiotensin-II. Crystallization and structure determination of hDPP III and IVYPW were performed by Manuel Reisinger. All structures, that are part of the project, were published in the journal Scientific reports [18].

For crystallization of hDPP III variants carrying several mutations were used. The protein was shortened by 11 amino acids on its C-terminal end, as this part of the protein was predicted to be unstructured [3]. Additional mutations were originally introduced by Prashant Kumar for utilization of the protein in single molecule Förster resonance energy transfer (smFRET) experiments: C19S, C519S, C654S, E207C and S491C. Crystallization trials were done with active and inactive hDPP III, the protein was rendered inactive by exchange of Glu-451 with Ala [2]. Variants used for crystallization will be referred to as „active hDPP III" and „inactive hDPP III" in this thesis.

Crystallization trials with mouse DPP III (mDPP III) were conducted with a C-terminally truncated variant of the protein. 11 amino acids were removed, that were assumed to be unstructured due to high similarity of the protein to hDPP III.

ITC experiments were conducted with shortened hDPP III (1-726), carrying the E451A mutation and thereby rendered inactive.

Fluorescent activity assays were done with wild type hDPP III (wtDPP III) and active shortened hDPP III (1 – 726) containing following mutations: C19S, C519S, C654S, E207C and S491C. Additionally, Phe-373 was mutated to Leu by site-directed mutagenesis. Therefore this variant will be referred to as „hDPP III F373L" in this thesis.

2. Materials and methods

2.1 Cloning and site-directed mutagenesis

All genes used in the experiments were ordered from Thermo Fisher Scientific in a pET28-MHL vector, with an N-terminal His_6-Tag attached, followed by a Tobacco Etch Virus (TEV) cleaving site and the protein sequence, optimized for expression in *Escherichia coli*. Site-directed mutagenesis was used to shorten the gene of mDPP III by 11 amino acids via introduction of a stop-codon. A mutation in the sequence of active hDPP III was introduced (F373L mutation) for utilization of the newly created variant in fluorescent activity assay experiments. Primers used for site-directed mutagenesis are listed in table 1.

Table 1: Primers used for site-directed mutagenesis of mDPP III and hDPP III F373L

mDPP III	
Forward primer	AGGTGCTTCTTGTGCCTGATTTTACCAAAAACGTGCATCTGCTGC
Reverse primer	GCAGCAGATGCACGTTTTTGGTAAAATCAGGCACAAGAAGCACCT
hDPP III F373L	
Forward primer	CGTCCAGGCTAGTGAGGTCCGGAGTCAGG
Reverse primer	CCTGACTCCGGACCTCACTAGCCTGGACG

50 µL PCR reaction mixtures were prepared to introduce the mutations. A primer concentration of 1 µM, dNTPs in a concentration of 200 µM and 1x Quick-solution (Thermo Fisher) were used. 1 ng of template DNA and 1 µL of Phusion Polymerase (20 000 U/mL, Thermo Fisher) were added. Two 50µL reaction mixtures were prepared, with forward and reverse primer respectively. After 4 PCR cycles (table 2) 25 µL of each reaction mixture were combined to create a 50 µL reaction mixture containing both primers. 18 PCR cycles were performed with this mixture. 1.5 µL of DpnI (20 000 U/mL) were added to the PCR product and incubated at 37°C for 2 h.

Table 2: Thermocycler program used for site-directed mutagenesis

	Temperature [°C]	**Duration [sec]**
Initial denaturation	95	55
Denaturation	95	55
Primer annealing	60 (mDPP III) 58 (F373L mutant)	55
Elongation	72	480
Final extension	72	480
Storage	4	∞

10 – 50 ng of DpnI digested PCR-product were added to 200 µL of competent cells (*E. coli* Top 10) and incubated at 4°C for 30 min. Thereafter the cells underwent heat shock treatment (90 sec, 42°C) and incubation on ice for 5 min, followed by addition of 700 µL autoclaved LB medium and incubation at 37°C for 50 min. For plating the cell suspension was spun and 600 µL of supernatant were taken off. Cells were resuspended in remaining medium and spread on LB agar plates containing 50 µg/mL Kanamycin. Agar plates were incubated at 37°C over night.

Several over night cultures (ONC) of 10 mL LB medium containing 50 µg/mL Kanamycin were created, each with one clone picked from an agar plate. ONCs were incubated at 37°C, shaking. Plasmids were isolated from those ONCs using the Qiagen MiniPrep kit according to protocol and analyzed by sequencing. One plasmid containing the desired sequence was introduced into expression cells (*E. coli* BL21 Codon Plus) by heat shock transformation. The same procedure as described for transformation into *E. coli* Top 10 cells was used and an ONC of 10 mL LB medium containing 50 µg/mL Kanamycin was made and incubated over night at 37°C, shaking. To create stock cells 650 µL of ONC were mixed with 350 µL of >86% autoclaved Glycerol. Stock cells were shock-frozen in liquid nitrogen and kept at -80°C.

2.2 Protein expression and purification

3 – 5 µL of stock cells were added to 10 mL of autoclaved LB medium containing 50 µg/mL Kanamycin and incubated at 37°C over night, shaking. 3 mL of pre-warmed ONC were used to inoculate a flask containing 700 mL autoclaved LB medium and 50 µg/mL Kanamycin. Several flasks were incubated at 37°C, shaking, until a OD_{600} of 0.5 – 0.8 was reached. Protein expression was then induced with 0.4 mM Isopropyl-β-D-thiogalactopyranosid (IPTG). After induction the incubation temperature was changed 18°C and the flasks were incubated over night, shaking. Cells were harvested by pelleting at 6700 g for 20 min at 4°C. The cells were washed by resuspension with 100 mM NaCl, followed by centrifugation at 3000 g for 40 min at 4°C. Fluid was discarded and the pellets were stored at -80°C.

Cell pellets were dissolved in 50 mM Tris-HCl pH 8.0, 300 mM NaCl, 5 mM Imidazole and 1 mM Tris(2-carboxyethyl)phosphine (TCEP). Cell lysis was achieved by sonicating the cell suspension on ice at 50% intensity, pulse 4 for 5 min. The sonication process was repeated three times. Subsequently cell debris was removed by centrifugation at 36000 g for 60 min at 4°C. To prepare the sample for chromatography, the supernatant was filtered using syringe filters with 0.45 µm pore size.

Ni^{2+}-affinity chromatography was performed on two consecutive GE Healthcare His-trap FastFlow 5 mL columns, equilibrated with 50 mM Tris-HCl pH 8.0, 300 mM NaCl and 1 mM TCEP. After sample application the sample was washed with equilibration buffer for 5 column volumes (CV) and eluted by applying a raising concentration of Imidazole, up to 500 mM Imidazole. A fraction volume of 2 mL was used to collect the protein. Eluted fractions were analyzed by 12% sodium dodecyl sulfate polyacrylamide gel electrophoresis (SDS-PAGE).

For dialysis and His_6-tag cleavage by TEV protease, 100 µg of TEV protease per mg of protein were added to a pool of the fractions containing DPP III. Protein amount was determined via spectrophotometric measurement using NanoDrop. Dialysis was performed against 50 mM Tris-HCl pH 8.0 and 300 mM NaCl over night at 4°C for mDPP III. The Zn-ion in inactive hDPP III was chelated by dialysis against several buffers (table 3) containing EDTA and

Pyridine-2,6-dicarboxylic acid at 4°C during TEV cleavage [19]. After dialysis, another 100 µg of TEV protease were added per mg of protein and incubated for 1 h at room temperature.

Table 3: Buffers used for Zn-ion chelation

Duration	**Buffer composition**
3 h	50 mM Tris-HCl pH 8.0, 300 mM NaCl, 4 mM EDTA
3 h	50 mM Tris-HCl pH 8.0, 300 mM NaCl, 4 mM EDTA
3 h	50 mM Tris-HCl pH 8.0, 300 mM NaCl, 4 mM EDTA
3 h	50 mM Tris-HCl pH 8.0, 300 mM NaCl, 30 mM Pyridine-2,6-dicarboxylic acid
3 h	50 mM Tris-HCl pH 8.0, 300 mM NaCl, 30 mM Pyridine-2,6-dicarboxylic acid
3 h	50 mM Tris-HCl pH 8.0, 300 mM NaCl
Over night	50 mM Tris-HCl pH 8.0, 300 mM NaCl
2 h	50 mM Tris-HCl pH 8.0, 300 mM NaCl

Reverse affinity chromatography was performed on a GE Healthcare His-trap FastFlow 5 mL column, equilibrated with 50 mM Tris-HCl pH 8.0, 300 mM NaCl and 1 mM TCEP. The protein was collected in 4 mL fractions. After protein elution the column was washed with 50 mM Tris-HCl pH 8.0, 300 mM NaCl and 500 mM Imidazole. 12% SDS-PAGE was performed to analyze the fractions containing protein.

Anion exchange chromatography was performed on a prepacked ResourceQ column (GE Healthcare), equilibrated with 20 mM Tris-HCl pH 8.0. Pooled fractions containing DPP III from affinity chromatography were diluted with anion exchange equilibration buffer to reach a NaCl concentration of 100 – 150 mM. After applying the sample to the column, a washing step with equilibration buffer was done for 5 CV. The protein was eluted by applying a raising concentration of NaCl, up to 1 M. A fraction volume of 0.5 mL was used

to collect protein. Protein containing fractions were analyzed by 12% SDS-PAGE.

Fractions containing DPP III were pooled and size exclusion chromatography was performed on a Superdex 200 26/60 gel filtration column (GE Healthcare) equilibrated with 100 mM multicomponent buffer (Tris, MES, malic acid) pH 8.0 [20], 150 mM NaCl. For collecting the protein a fraction size of 2 mL was chosen. The fractions were analyzed using 12% SDS-PAGE.

Fractions containing pure DPP III were pooled and concentrated at 3000 g using a centricon with 30 kDa pore size. The protein was used for crystallization directly after purification.

2.3 Protein crystallization trials

Freshly purified protein was used for all crystallization trials. To dissolve precipitations the protein was centrifuged at 16000 g for 15 min. Precipitations in the ligands used for cocrystrallization were dissolved by a short spin. A sitting drop vapor diffusion setup at 20°C was used for protein crystallization. All crystallization approaches were performed with protein and ligand in 100 mM multicomponent buffer with 150 mM NaCl. Protein concentrations of 8 mg/mL, 10 mg/mL and 12 mg/mL were used for all crystallization trials of hDPP III. 0.056 M sodium phosphate monobasic monohydrate, 1.344 M potassium phosphate dibasic pH 8.2 (Index #19, Hampton Research) was used as reservoir [3]. A drop size of 1.2 µL was chosen for all crystallization experiments. For cocrystallization 0.6 µL of protein and ligand in multicomponent buffer and 0.6 µL of reservoir were used. For cocrystallization of inactive hDPP III and angiotensin-II a protein-ligand-ratio of 1+30 was chosen. Crystals were grown for two months and then flash-cooled to 100 K without additional cryoprotectant.

For further crystallization attempts, seeds were made from crystals of inactive hDPP III in complex with angiotensin-II. Seeding stock was produced by crushing the crystals with a probe and transferring them to a test tube containing a seed bead and 50 µL of condition Index #19 (Hampton Research). The test tube was vortexed for 2 min, pausing every 30 sec to cool

it on ice. For cross-seeding experiments 0.6 µL of protein and ligand in multicomponent buffer, 0.4 µL of reservoir and 0.2 µL of seeding stock were used.

For cocrystallization of inactive hDPP III with valorphin a protein-ligand-ratio of 1+50 was used. Crystallization of inactive hDPP III in complex with endomorphin-2 was attempted with protein-ligand-ratios of 1+5, 1+10 and 1+30. Cocrystallization trials with leu-enkephalin and met-enkephalin were done with protein-ligand-ratios of 1+10, 1+20, 1+30 and 1+40. For cocrystallization trials of inactive hDPP III with AAβNA a protein-ligand-ratio of 1+40 was chosen. Crystals were grown one month and then flash-cooled to 100 K without additional cryoprotectant.

For crystallization of mDPP III protein concentrations of 8 mg/mL, 10 mg/mL and 12 mg/mL were used. A drop size of 1.2 µL was chosen, with 0.6 µL protein in 100 mM Multicomponent buffer with 150 mM NaCl and 0.6 µL reservoir. Screening experiments were conducted with Index Screen, PEG/Ion Screen, Morpheus Screen, Crystal Screen, SaltRX Screen, JCSG Screen and Midas Screen.

Furthermore, cross-seeding experiments were done using seeds produced from crystals of inactive hDPP III in complex with angiotensin-II. A drop size of 1.2 µL was chosen, with a composition of 0.6 µL protein in 100 mM Multicomponent buffer with 150 mM NaCl, 0.4 µL reservoir and 0.2 µL seeding stock. mDPP III was used in a concentration of 8 mg/mL. The cross-seeding experiments were conducted using Index Screen and Morpheus Screen.

2.4 Protein structure determination

The diffraction dataset for inactive hDPP III in complex with angiotensin-II was collected at beamline BM14 (ESRF Grenoble), the structure was refined by Prashant Kumar. The diffraction datasets for inactive hDPP III in complex with met-enkephalin and in complex with endomorphin-2 were gathered ID29 (ESRF Grenoble).

For initial data reduction and processing the program XDS was used. Molecular replacement was carried out in PHASER. As a search model the structure of

tynorphin bound hDPP III at 2.4 Å resolution was used [3]. Structures were refined using PHENIX. Model fitting and real space refinement were done in the program COOT.

2.5 Fluorescent activity assay

Protein activity of wtDPP III and hDPP III F373L were measured by a standard fluorescent activity assay, as described by *Jajčanin-Jozić et al.* [21] at a temperature of 37°C. A protein concentration of 500 pM was chosen for measuring the activity of hDPP III F373L. For activity measurement of wtDPP III a protein concentration of 20 pM was chosen. AAβNA was used as a substrate in a range of concentrations between 0.5 µM to 500 µM. Protein and substrate were dissolved in 50 mM Tris-HCl pH 8.0 and 150 mM NaCl. To detect β-naphthylamide (βNA), the product of enzymatic reaction, an excitation wavelength of 340 nm and an emission wavelength of 420 nm were used. The slitwidth was set to 4 µm. The fluorescence of βNA was measured for concentrations from 0.01 µM to 2 µM to create a calibration curve. The calibration curve relates absorbance of βNA to the concentration of product. It was used to calculate enzyme velocity in pM/s. K_M, K_{cat} and V_{max} were determined using GraphPad Prism 5.

2.6 Isothermal titration calorimetry (ITC)

A VP-ITC microcalorimeter (MicroCal, Northampton, MA, USA) was used to measure microcalorimetric data for hDPP III E451A and angiotensin-II. Protein and ligand were dissolved in 50 mM Tris-HCl pH 8.0 and 100 mM NaCl. A protein concentration of 40 µM was chosen for the measurement. The data was recorded using a ligand concentration of 800 µM. Protein and ligand solution were degassed before the measurement was started.

The microcalorimeter was calibrated to 25°C. A total of 30 ligand aliquots were injected into 1.421 mL of protein solution, the first aliquot of 2 µL, then 29 aliquots of 10 µL. The protein solution was constantly stirred at 270 rpm. A spacing of 225 sec between every injection was chosen.

A reference measurement was taken with 800 μM angiotensin-II in the same manner and was used to correct for the heat of dilution of the peptide. Data analysis was performed in Origin software, nonlinear least-squares fitting was used to calculate association constants (K_a), heats of binding (ΔH) and stoichiometry. Gibbs free energy (ΔG) and entropy of binding (-TΔS) were calculated using the Gibbs-Helmholtz equation.

3. Results

3.1 Site-directed mutagenesis

Site-directed mutagenesis was used to shorten mDPP III to a lenght of 726 amino acids and to exchange Phe 373 with Leu in active hDPP III. mDPP III was then used in crystallization trials, the hDPP III F373L variant was created for utilization in fluorescent activity assays. The newly created vectors were sequenced and compared with the original sequence by performing a sequence alignment. The sequences were aligned using ClustalOmega, an alignment tool provided by EMBL-EBI.

Figure 3 shows the part of the sequence alignment of modified and original sequence of the mDPP III gene in pET 28-MHL, where the mutation was introduced. 2179-CGT-2181 in the original sequence was replaced by 2179-TAA-2181, which acts as a stop codon. The expressed protein is a shortened mDPP III variant (1 – 726).

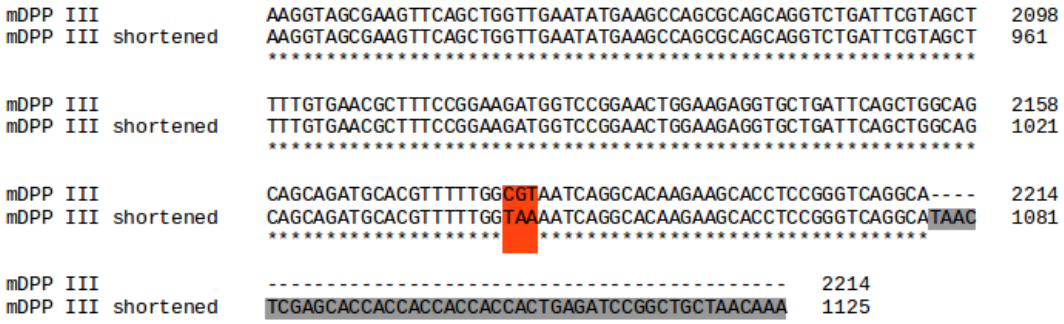

Figure 3: Partial sequence alignment of mDPP III and shortened mDPP III

The original sequence of mDPP III (codon-optimized for expression in *E. coli*) is labeled as „mDPP III", the mutated sequence is labeled as „mDPP III shortened". The nucleotides exchanged by site-directed mutagenesis are highlighted red, the sequence highlighted grey is part of the pET 28-MHL vector. CGT was changed to the stop codon TAA in order to shorten the protein for 11 amino acids.

In figure 4 the part of the sequence alignment, where the mutation in active hDPP III was introduced, is shown. 1117-TTC-1119 in the original sequence, which encodes Phe 373, was replaced by 1117-CTC-1119, which encodes Leu.

Figure 4: Partial sequence alignment of active hDPP III and hDPP III F373L

The original sequence of active hDPP III (codon-optimized for expression in *E. coli*, containing smFRET mutations) is labeled as „active hDPP III", the mutated sequence is labeled as „F373L". The base triplet, that was targeted by site-directed mutagenesis, is highlighted red. TTC was exchanged with CTC to exchange Phe with Leu.

3.2 Protein purification

Protein expression was performed over night at 18°C. Cells were harvested, washed and pelleted. Cell lysis was achieved by sonication. After filtration of the sample purification by Ni^{2+}-affinity chromatography was performed. SDS-PAGE was conducted to analyze fractions with high protein amount. The Coomassie-stained gel is shown in figure 5. DPP III has a size of 82 kDa. A strong band at a size of around 80 kDa can be observed on the gel in several fractions. Therefore it can be concluded that a vast amount of protein was expressed. However, also a lot of other bands can be seen on the gel. These impurities were removed by further purification steps.

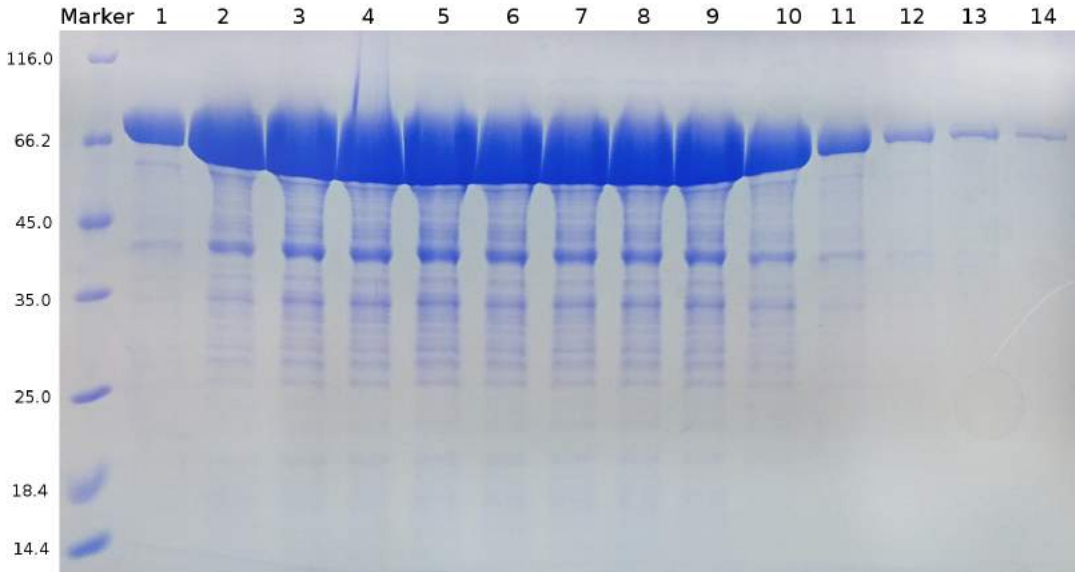

Figure 5: Affinity chromatography, Coomassie-stained gel

Protein containing fractions were analyzed by SDS-PAGE after affinity chromatography. Thermo Scientific Pierce unstained protein molecular weight marker was used as a standard. hDPP III has a size of 82 kDa, a strong band can be seen in fractions 1 to 11 referring to this size. In fractions 12 to 14 the band is weaker. A high amount of other proteins can be seen on the gel.

After Ni^{2+}-affinity chromatography fractions containing DPP III were pooled and left for TEV cleavage and dialysis over night. Subsequently reverse affinity chromatography was performed. The flow-through contained a high amount of protein and were analyzed by 12% SDS-PAGE, as well as three fractions eluted by 100% elution buffer. The gel was stained with Coomassie blue, a picture of the gel is shown in figure 6. Fractions 1 to 11 contain proteins, that did not bind to the column. A strong band can be seen in those fractions referring to a size of around 80 kDa, this band is created by DPP III that does not have the His_6-Tag attached anymore. Several bands correlated to proteins of other sizes can be observed. To get pure DPP III for utilization in crystallization trials, impurities were removed by further purification steps. The last few fractions (fractions 12 - 14) show proteins eluted by 100% elution buffer. In those fractions TEV protease (27 kDa) can be found, because it contains a His_6-Tag and therefore bound to the column. Moreover, a strong band at around 80 kDa can be seen in those fractions. They relate to DPP III, that was not cleaved by TEV protease and still has the His_6-Tag attached.

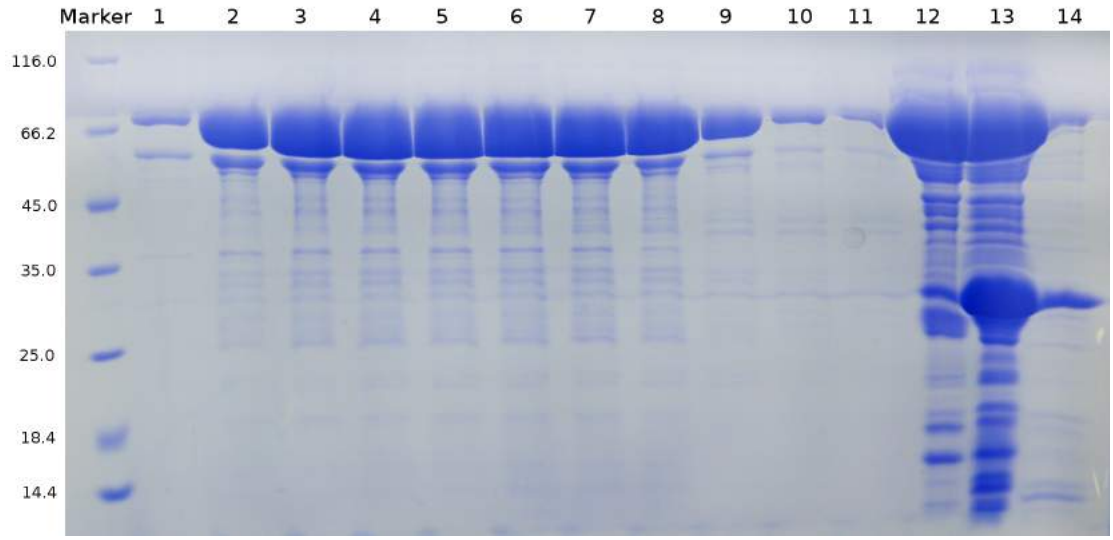

Figure 6: Reverse affinity chromatography, Coomassie-stained gel

Fractions containing protein were analyzed by SDS-PAGE. Thermo Scientific Pierce unstained protein molecular weight marker was used as a standard. Fractions 1 to 11 show the collected flow-through and contain a high amount of hDPP III and some impurities. Fractions 12 to 14 were eluted using 100% elution buffer. hDPP III still having the His_6-Tag attached is eluted in those fractions, as well as TEV protease (27 kDa) and impurities.

Anion exchange chromatography was performed using fractions 1 to 11 from reverse affinity chromatography, which were pooled and diluted with 20 mM Tris-HCl pH 8.0 to reach a concentration of 100 – 150 mM NaCl. After chromatography SDS-PAGE was used to evaluate which fractions contain DPP III. The Coomassie-stained gels are shown in figure 7 and 8. Again, a strong band correlated to a size of around 80 kDa and some other weak bands can be seen. DPP III is relatively pure after anion exchange chromatography. Nevertheless, for higher purity and thereby higher probability to gain crystals, size exclusion chromatography was carried out.

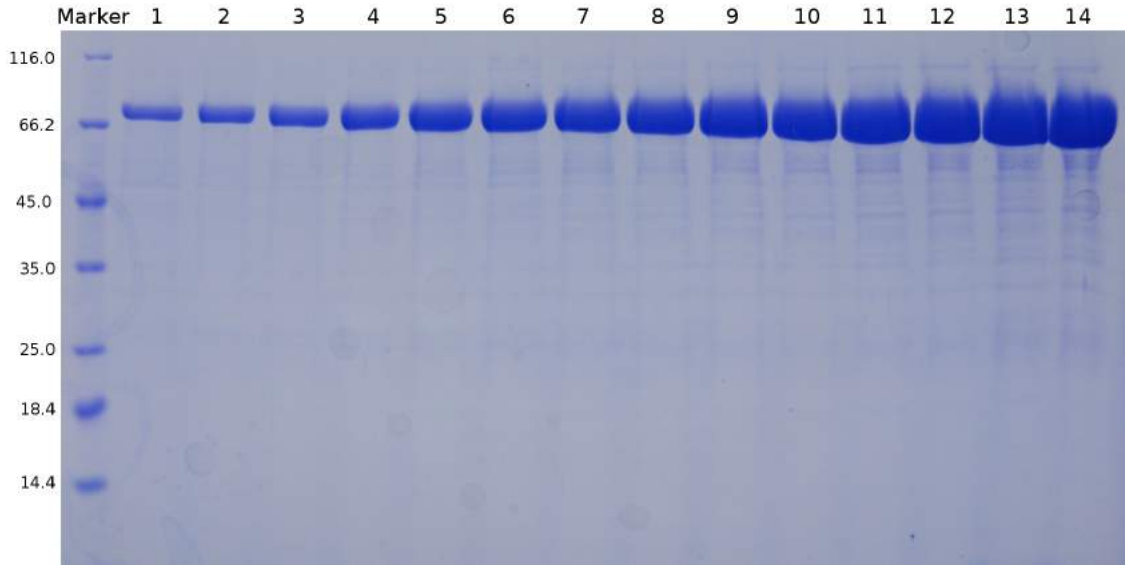

Figure 7: Anion exchange chromatography, Coomassie-stained gel 1

Protein containing fractions from anion exchange chromatography were analyzed using SDS-PAGE. As a standard Thermo Scientific Pierce unstained protein molecular weight marker was used. All fractions analyzed contain a high amount of hDPP III and some impurities.

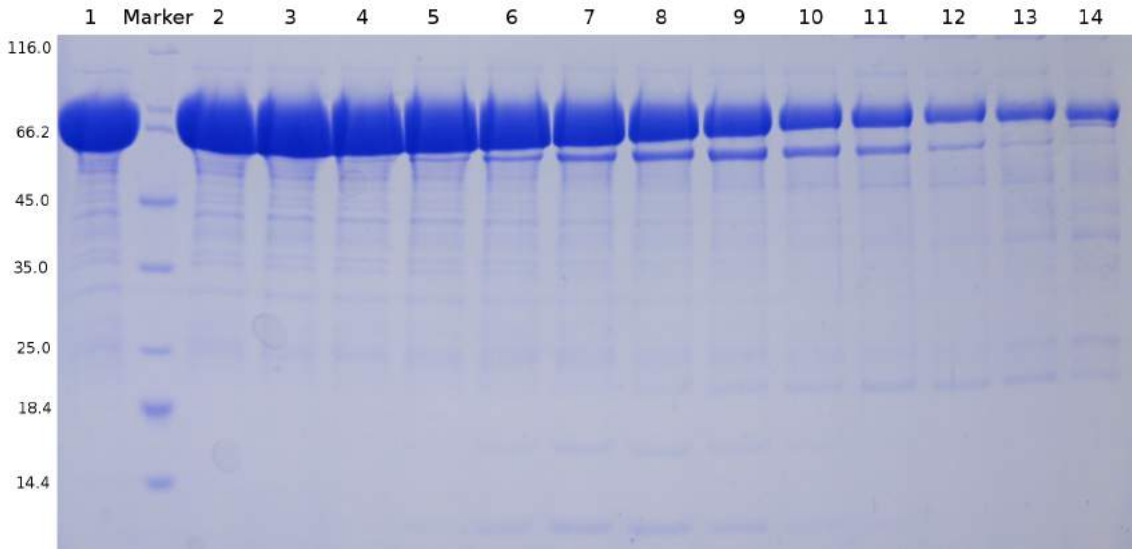

Figure 8: Anion exchange chromatography, Coomassie-stained gel 2

Fractions containing protein from anion exchange chromatography were analyzed. Thermo Scientific Pierce unstained protein molecular weight marker was used as a standard. All fractions contain a high amount of hDPP III and some impurities. In fractions 6 to 13 a strong band can be seen at a height of around 55 kDa, this band can be interpreted as a degradation product of hDPP III.

Protein containing fractions from size exclusion chromatography were analyzed by SDS-PAGE, the gel was stained with Coomassie blue and is shown in figure 9. Fractions 2 to 10 contain DPP III. Other very weak bands can be recognized, but DPP III is already very pure after this purification step and can be used for crystallization trials.

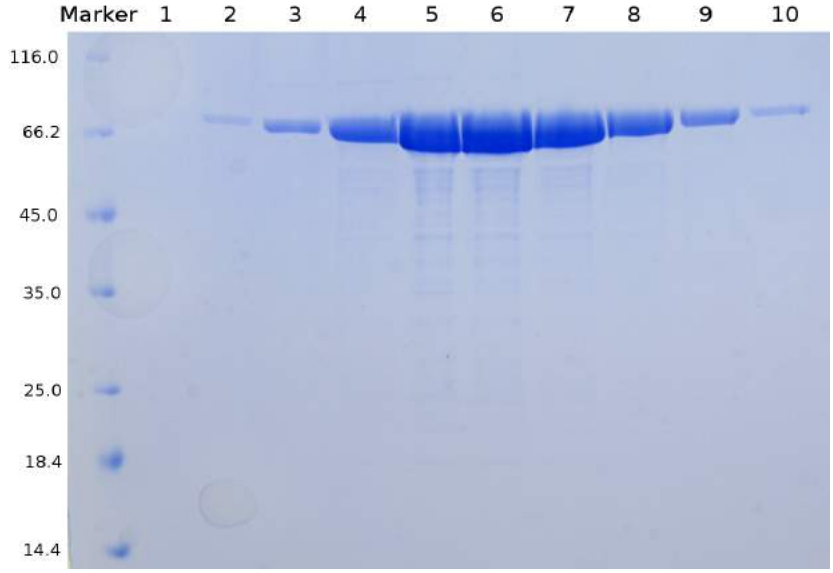

Figure 9: Size exclusion chromatography, Coomassie-stained gel

Thermo Scientific Pierce unstained protein molecular weight marker was used as a standard. Fractions 2 to 10 contain hDPP III. There is a low amount of impurities visible.

3.3 Protein structure determination

Crystals of inactive hDPP III in complex with several ligands were obtained in a sitting drop vapor diffusion setup at 20°C. Freshly purified protein was used for all crystallization trials. A drop size of 1.2 µL composed of 0.6 µL protein and ligand in Multicomponent buffer and 0.6 µL condition Index #19 was used for cocrystallization of inactive hDPP III and angiotensin-II. Crystals were obtained with 8 mg/mL protein and a protein-ligand-ratio of 1+30.

1.2 µL drops composed of 0.6 µL protein and ligand in Multicomponent buffer, 0.4 µL condition Index #19 and 0.2 µL seeding stock (made from crystals of inactive hDPP III in complex with angiotensin-II) were used for further crystallization experiments. A protein concentration of 8 mg/mL yielded to

crystals of hDPP III in complex with met-enkephalin or endomorphin-2, a protein-ligand-ratio of 1+30 was used. All crystals obtained show the same morphology (figure 10). Crystallization trials with mDPP III did not yield any crystals.

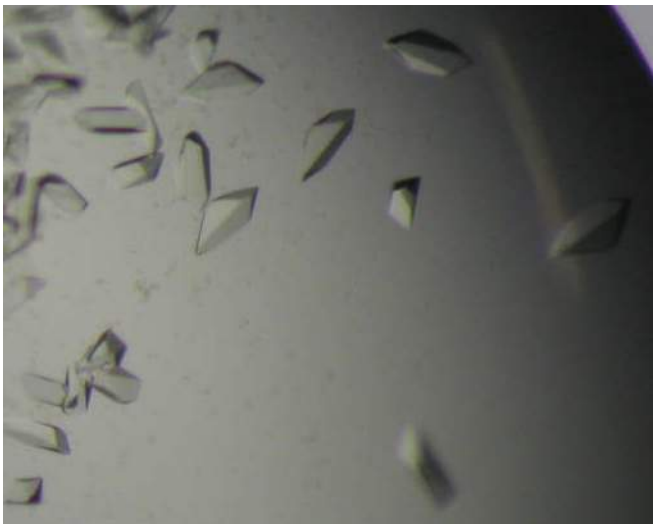

Figure 10: hDPP III crystals

Crystals of hDPP III in complex with met-enkephalin are shown in the picture. Crystallization of hDPP III with other ligands resulted in crystals with same morphology.

The crystals obtained were monoclinic (space group C2) with one molecule per asymmetric unit. The crystals of inactive hDPP III in complex with met-enkephalin and endomorphin-2 diffracted to 1.85 Å and 2.38 Å resolution respectively. The structure of inactive hDPP III in complex with angiotensin-II was determined by Prashant Kumar. Data collection and refinement statistics for the structure of inactive hDPP III in complex with met-enkephalin or endomorphin-2 are summarized in table 4.

Table 4: Crystallographic data and refinement statistics

	hDPP III + Met-enkephalin	hDPP III + Endomorphin-2
Crystal Parameters		
Program	XDS	XDS
Synchrotron	ESRF ID29	ESRF ID29
Space Group	C 1 2 1	C 1 2 1
Unit Cell parameters [Å,°]	119.79, 105.76, 65.167, 90, 93.49, 90	120.035, 105.457, 64.719, 90, 93.49, 90
Data Collection		
Resolution [Å]	45.42-1.84 (1.90-1.84)	49.09-2.378 (2.463-2.378)
Wavelength [Å]	0.972	0.972
R_{merge} [%]	0.0505 (0.7368)	0.09141 (0.632)
R_{meas} [%]	0.0601	0.1084
<I/δ(I)>	14.78 (1.75)	10.61 (1.78)
R_{pim}	0.033 (0.55)	0.058 (0.377)
Total number of reflections	231251 (22436)	110082 (10317)
No. of unique reflections	68276 (6626)	32020 (3068)
Multiplicity	3.4 (3.4)	3.4 (3.4)
Completeness [%]	96.89 (93.80)	98.87 (95.37)
Wilson B factor	30.13	40.63
$CC_{1/2}$	0.999 (0.63)	0.996 (0.66)
CC*	1 (0.87)	0.999 (0.89)
Refinement		
R_{work} [%]	0.181	0.19
R_{free} [%]	0.223	0.23
Bond lengths [Å]	0.011	0.005
Bond angles [°]	1.23	0.71
Clash score	5.82	4.37
No. Of non-hydrogen atoms	6339	6059
Ligands	4	4
Protein residues	726	726
No. Of water molecules	519	270
Average B factor [$Å^2$]	37.00	37.4
Macromolecule	37.10	37.6
Ligands	28.50	30.0
Solvent	37.00	32.5
Ramachandran analysis		
Favored [%]	98	97
Allowed [%]	1.86	3
Disallowed [%]	0.14	0

3. 3. 1 hDPP III in complex with met-enkephalin

Met-enkephalin (YGGFM) is a pentapeptide involved in nociception. Because DPP III shows a high in vitro affinity to enkephalins, it is also referred to as enkephalinase B [1]. The structure of inactive hDPP III and met-enkephalin was determined at 1.85 Å resolution.

The overall structure of hDPP III in complex with met-enkephalin is shown in figure 11. The protein is present in its closed conformation, it has an almost globular shape and the ligand is completely buried in the binding site. This conformation was also observed in the structure of hDPP III in complex with tynorphin [3].

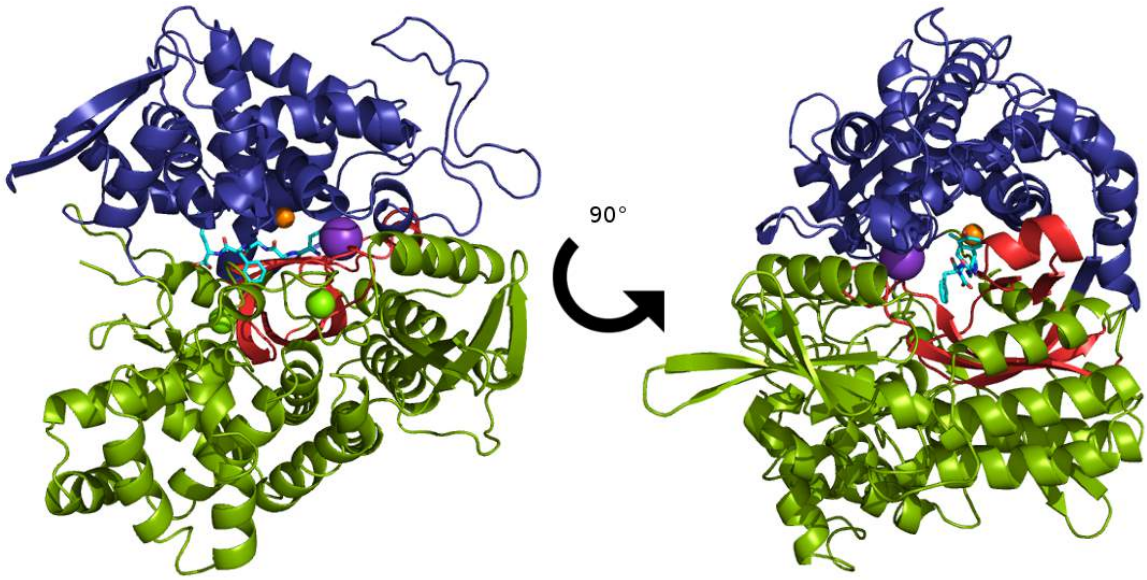

Figure 11: Overall structure of inactive hDPP III in complex with met-enkephalin

The structure of inactive hDPP III in complex with met-enkephalin is shown in two different orientations. The upper lobe of the protein is colored blue, the lower lobe is colored green, the 5-stranded β-core is shown in red. Met-enkephalin is shown in cyan, the Zn-ion as a orange sphere, the K-ion as a purple sphere and Mg-ions are pictured as green sphere.

Interactions between hDPP III and met-enkephalin are pictured in figure 12. The N-terminus of met-enkephalin is anchored to the protein by several hydrogen bonds provided by the 5-stranded β-core of hDPP III (Ala-388 to Asn-391) and hydrogen bonds with Asn-394, Glu-316 and Tyr-318. Moreover,

an interaction is formed between the conserved His-568 and the ligand. Because extensive interactions between protein and ligand are formed, the N-terminal end of met-enkephalin is able to bind as an extended β-strand, despite the presence of glycine residues. The C-terminus of met-enkephalin interacts with Arg-669 via a salt bridge.

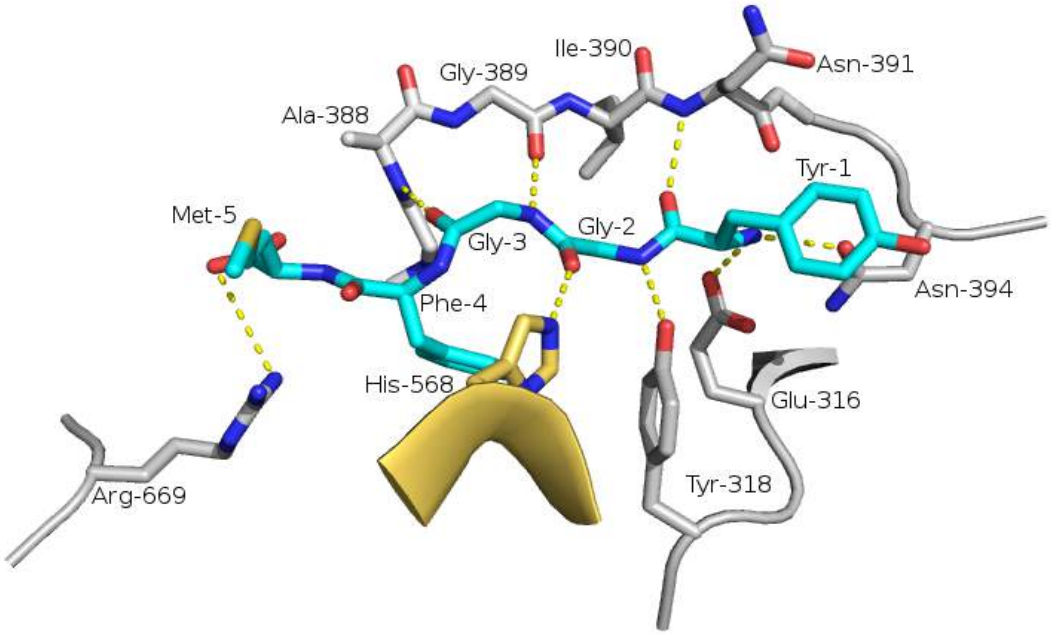

Figure 12: Interactions of inactive hDPP III with met-enkephalin

Met-enkephalin is shown in cyan, the upper lobe of hDPP III is colored yellow and the lower lobe of the protein is shown in gray. Interactions are pictured as yellow dashed lines.

The electron density of met-enkephalin bound to hDPP III (shown in figure 13) coincides with the binding mode. On the N-terminus of the peptide the electron density is well defined, here the ligand is anchored in the binding site of hDPP III by several interactions. In contrast, the lower electron density on the C-terminal end of met-enkephalin indicates this part of the ligand is more flexible.

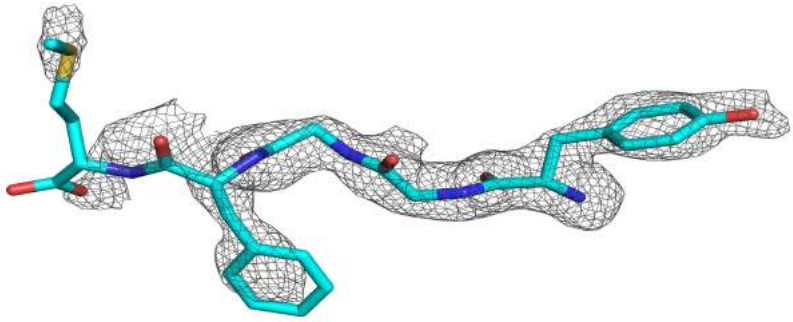

Figure 13: Electron density of met-enkephalin bound to hDPP III (reused from [18])

Met-enkephalin is shown in cyan with the Fo-Fc map contoured at 2.5 σ (gray).

3. 3. 2 hDPP III in complex with endomorphin-2

Endomorphin-2 (YPFF-NH_2) is an endogenous opioid peptide with an amidation on its C-terminus [1]. A crystal structure of hDPP III in complex with endomorphin-2 was determined at a resolution of 2.38 Å.

The overall structure of hDPP III in complex with endomorphin-2 is shown in figure 14. The protein is present in its closed conformation, which was also observed in the structures of hDPP III in complex with tynorphin [3] or met-enkephalin.

Figure 15 shows interactions between hDPP III and endomorphin-2. The N-terminus of the peptide is anchored by polar interactions formed with residues from the 5-stranded β-core (Ala-388 to Asn-391), as well as Glu-316, Asn-394, Arg-399 and Arg-669 from the lower lobe of the protein. Despite forming extensive interactions with hDPP III, endomorphin-2 does not bind as a β-strand to the protein. The ligand cannot form a β-strand, because its second amino acid is a Pro. Arg-572 from the upper lobe of hDPP III interacts with endomorphin-2. Interestingly, endomorphin-2 also interacts with the catalytic Zn-ion. This interaction was not observed in the structures of hDPP III in complex with angiotensin-II, met-enkephalin and leu-enkephalin. Furthermore, the distance between His-568 and the P1 carbonyl of the peptide is 3.7 Å. His-568 was found to interact with all other ligands bound to hDPP III and is proposed to stabilize the oxyanion intermediate formed during substrate hydrolysis [2, 3].

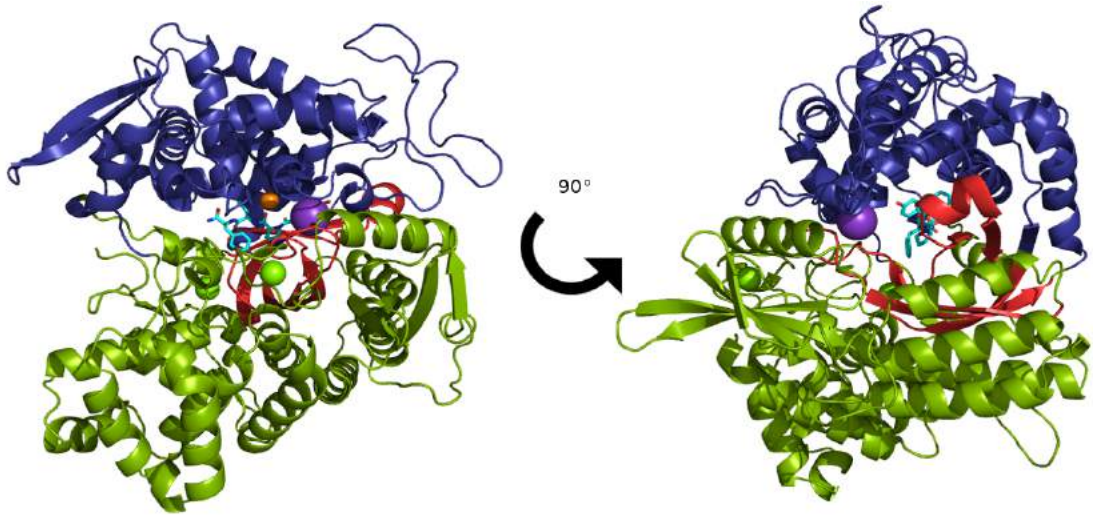

Figure 14: Overall structure of inactive hDPP III in complex with endomorphin-2

The structure of inactive hDPP III in complex with endomorphin-2 is shown in two different orientations. The upper lobe of the protein is colored blue, the lower lobe is colored green, the 5-stranded β-core is shown in red. Endomorphin-2 is shown in cyan, the Zn-ion as a orange sphere, the K-ion as a purple sphere and Mg-ions are pictured as green sphere.

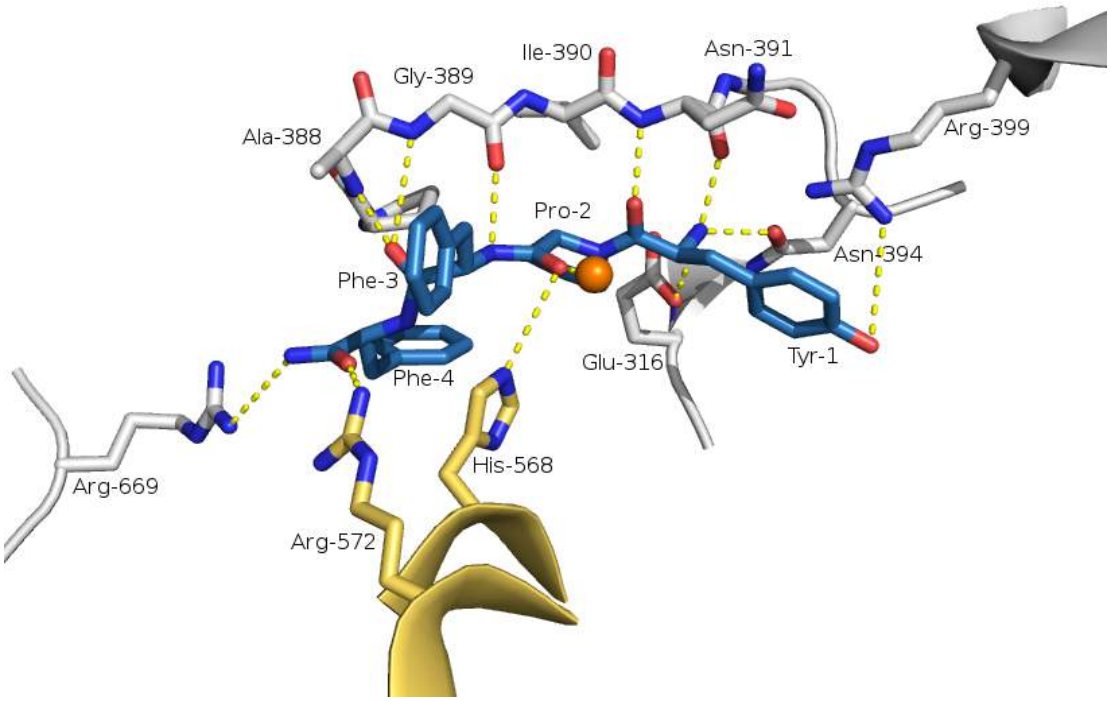

Figure 15: Interactions of inactive hDPP III with endomorphin-2

Endomorphin-2 is shown in blue, the upper lobe of hDPP III is colored yellow and the lower lobe of the protein is shown in gray. Interactions are pictured as yellow dashed lines. The Zn-ion is pictured as a orange sphere.

The electron density of endomorphin-2 bound to hDPP III (shown in figure 16) seems well defined on the N-terminus and C-terminus of the ligand. However, the middle part of the peptide lacks observable electron density. Moreover, an occupancy of less than 100% was observed. Those restrictions were considered when the structures of hDPP III in complex with ligands were interpreted.

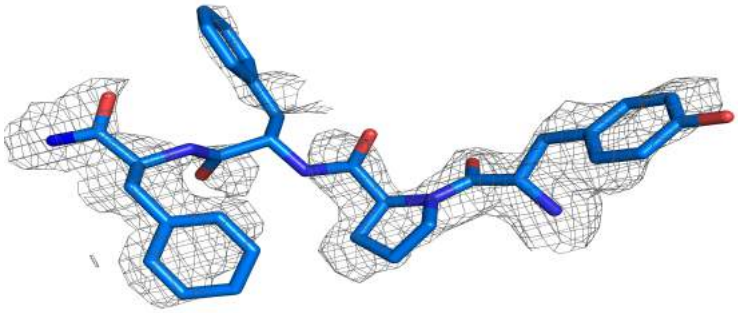

Figure 16: Electron density of endomorphin-2 bound to hDPP III (reused from [18])

Endomorphin-2 is colored blue with the Fo-Fc map contoured at 2.5 σ (gray).

3.4 Fluorescent activity assay

Data obtained in activity measurements was analyzed in GraphPad Prism 5. Figure 17 shows the Michaelis-Menten kinetics for wtDPP III and hDPP III F373L. Kinetic parameters for wtDPP III and hDPP III F373L are shown in table 5. K_M did not change upon mutation of Phe 373 to Leu, K_{cat} is reduced nearly 20-fold.

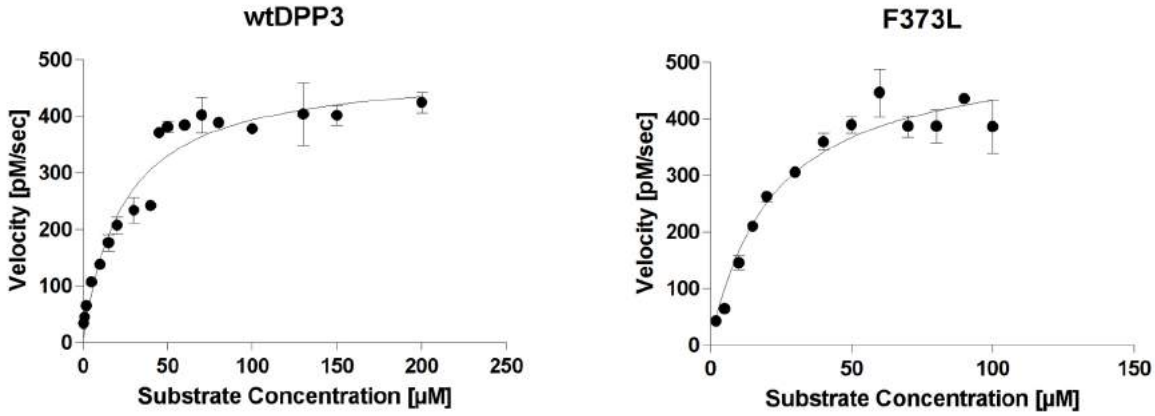

Figure 17: Michaelis-Menten kinetics of wtDPP III and hDPP III F373L

The Michaelis-Menten saturation curve of wtDPP III is shown on the left, the curve for hDPP III F373L is shown on the right. The curves were created using GraphPad Prism 5.

Table 5: Enzyme kinetics of wtDPP III and hDPP III F373L

Protein	**V_{max} (pM/sec)**	**K_M (µM)**	**K_{cat} (sec^{-1})**
wtDPP III	486.2 ± 21.2	23.6 ± 3.5	24.3 ± 1.1
hDPP III F373L	526.0 ± 28.2	21.7 ± 3.6	1.1 ± 0.1

3.5 Isothermal titration calorimetry (ITC)

A protein concentration of 40 µM and a ligand concentration of 800 µM were used for ITC measurements. Data was analyzed in Origin software using nonlinear least-squares fitting. Heat of dilution was corrected by subtracting reference measurement data.

Figure 18 shows the data obtained by ITC measurement depicted as peaks and the peak integral as a function of molar ratio of hDPP III E451A and angiotensin-II. Each peak refers to one injection, the energy needed to maintain the sample cell at a constant temperature is plotted on the y-axis. Thermodynamic parameters calculated in Origin software are shown in table 6.

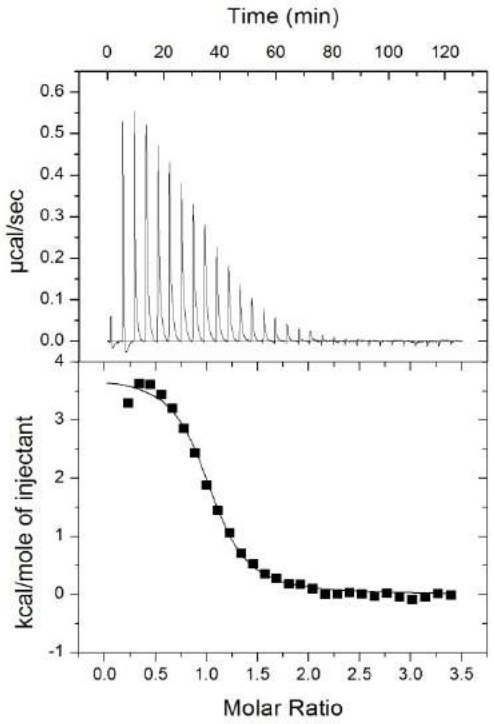

Figure 18: ITC of inactive hDPP III and angiotensin-II

The evolution of heat for each injection is shown in the upper part of the picture, the bottom shows the peak integral as a function of molar ratio of inactive hDPP III to angiotensin-II. A solid curve was used to picture the best fit using a one binding site model.

Table 6: Thermodynamic parameters of inactive hDPP III and angiotensin-II

Thermodynamic parameter	Value
K_d [µM]	1.64 ± 0.12
ΔH [kJ·mol^{-1}]	15.25 ± 0.17
ΔG [kJ·mol^{-1}]	-32.93 ± 0.18
-TΔS [kJ·mol^{-1}]	-48.18 ± 0.24

4. Discussion

4.1 Structures of hDPP III in complex with various ligands

DPP III has been shown to cleave peptides in a length ranging from 4 to 10 amino acids and with diverse amino acid compositions [1]. However, up to now only one structure of hDPP III in complex with a ligand has been reported and this structure differs substantially from the ligand-free structure. Ligand-free hDPP III is an elongated protein with an upper and a lower lobe, divided by a large cleft, which is proposed to be the ligand binding site. By comparison, tynorphin-bound hDPP III has an almost globular shape and the ligand is buried in the binding side. It is suggested, that the upper and lower lobe of the protein move towards each other as rigid bodies when the ligand binds [3]. However, it is still unclear how the protein is able to adapt to the different peptides it seems to accept and if other ligands induce a similar domain movement. This subject was investigated in this project by determining the structure of hDPP III in complex with several ligands (met-enkephalin, leu-enkephalin, IVYPW, endomorphin-2, angiotensin-II). The hDPP III variant used for crystallization was rendered inactive by exchange of the catalytic Glu-451 with Ala and carried several mutations originally introduced for utilization of the protein in smFRET experiments. Surprisingly, one of the introduced cysteine residues (Cys-207) was observed forming an intermolecular disulfide bridge in the crystal, which may have promoted crystallization (shown in figure 19).

The structures determined in this thesis (hDPP III in complex with met-enkephalin and hDPP III in complex with endomorphin-2) were analyzed along with the other structures, which were determined in this project by Prashant Kumar and Manuel Reisinger (hDPP III in complex with angiotensin-II, leu-enkephalin or IVYPW) [18]. A superposition of those ligand-bound structures of hDPP III is shown in figure 20. The protein is present in its closed conformation in all structures. This supports the hypothesis that a large conformational change is triggered upon ligand binding. The upper and the lower lobe of the protein move towards each other as rigid bodies and the ligand is completely buried inside the binding cleft.

Moreover, the structures are very similar and superimpose with an average rmsd of 0.235 Å, irrespective of length and amino acid composition of the ligand. This suggests that the protein does not undergo any structural changes in order to adapt to different ligands.

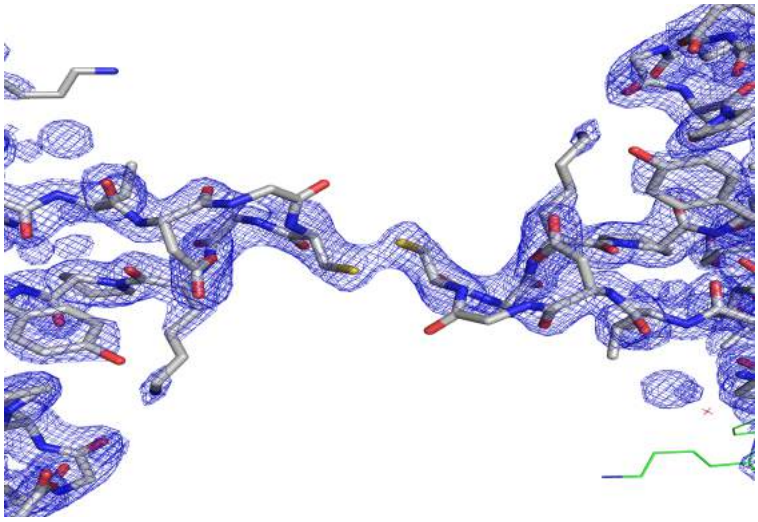

Figure 19: Intermolecular disulfide bridge (reused from [18])

The disulfide linkage, that was formed between the Cys-207 (originally introduced for smFRET experiments) of one molecule to the Cys-207 of its symmetry related molecule is shown. This interaction may have promoted crystallization.

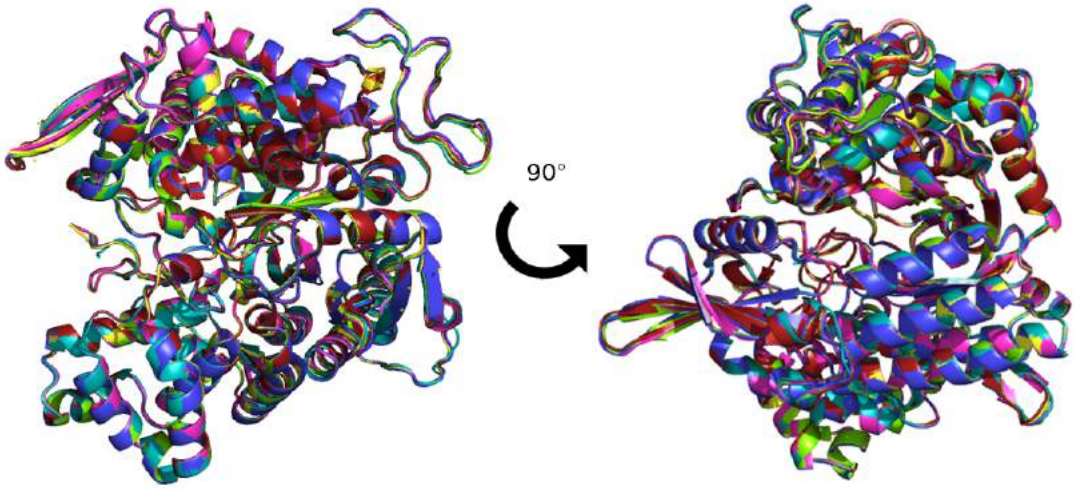

Figure 20: Superposition of ligand-bound hDPP III

A superposition of structures of hDPP III in complex with ligands is shown. hDPP III in complex with met-enkephalin colored pink, in complex with endomorphin-2 it is shown in green. hDPP III in complex angiotensin-II (PDB: 5E2Q) is colored red, with leu-enkephalin (PDB: 5E3A) yellow and the protein in complex with IVYPW (PDB: 5E3C) is colored blue [18].

A superposition of met-enkephalin, leu-enkephalin, endomorphin-2, angiotensin-II and IVYPW when bound to hDPP III is pictured in figure 21. The ligands superimpose very well on their N-terminal end. This is important, because the N-terminus of a substrate has to be positioned correctly to enable hDPP III to hydrolyze the scissile peptide bond. The C-terminal ends of the ligands show a greater variety in their conformation.

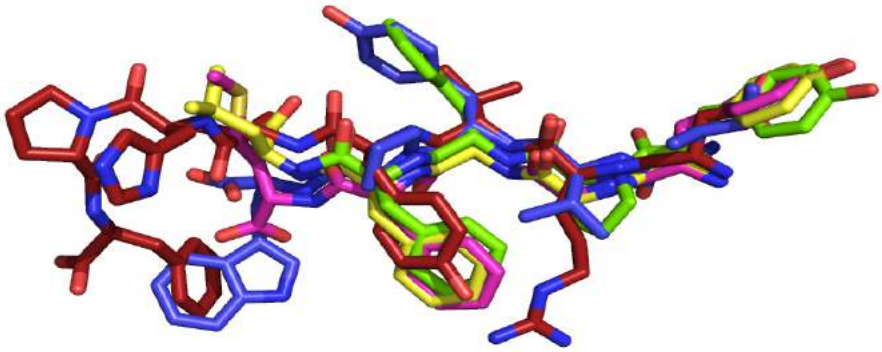

Figure 21: Superposition of ligands bound to inactive hDPP III (adapted from [18])

A superposition of met-enkephalin (pink), IVYPW (blue), angiotensin-II (red), leu-enkephalin (yellow) and endomorphin-2 (green) when bound to hDPP III is shown. The N-terminal ends of the ligands superimpose very well, the C-terminal ends are more variable.

4. 1. 1 hDPP III in complex with tynorphin

Interactions between hDPP III and tynorphin were described by *Bezerra et al.* and are shown in figure 22. The pentapeptide tynorphin is bound to the protein by polar interactions provided from residues of the lower lobe of hDPP III (Glu 316, Asn 394, Asn 391 and Tyr 318) and His-568 from the upper lobe. A salt bridge is formed between Arg-669 and the C-terminal carboxylate of the ligand. Several interactions are provided by the 5-stranded β-core of the protein. The ligand binds as an extended β-strand in a antiparallel fashion to the 5-stranded β-core of hDPP III [3]. A similar binding mode was also observed in the structures of hDPP III in complex with met-enkephalin, leu-enkephalin, endomorphin-2, angiotensin-II or IVYPW [18].

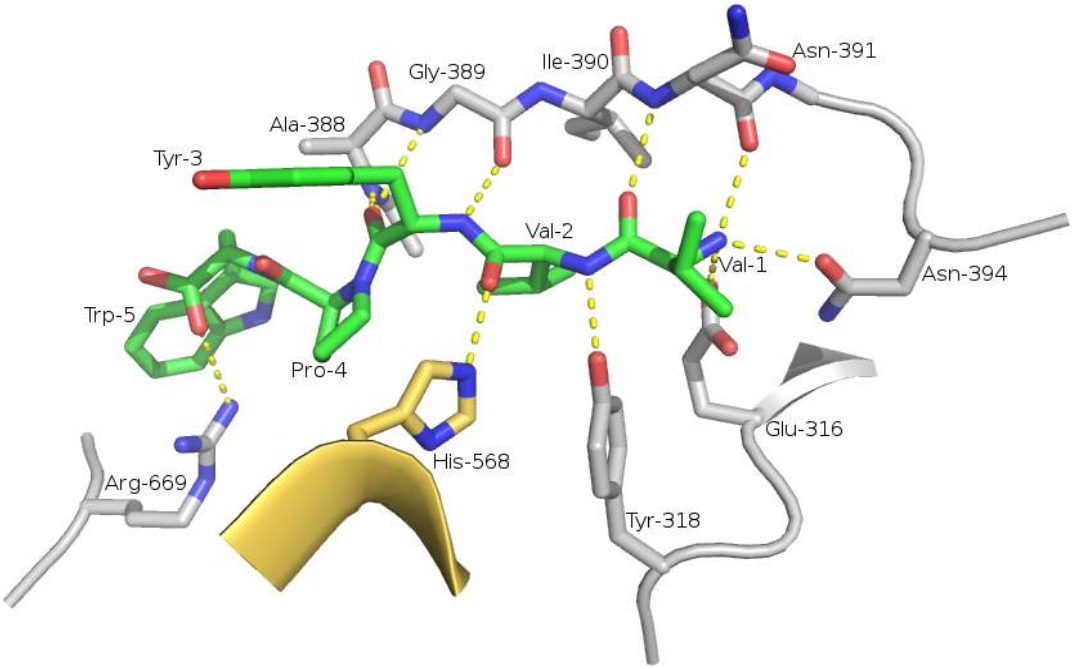

Figure 22: Interactions of hDPP III with tynorphin (adapted from [3], PDB: 3T6B)

Tynorphin is colored green, the upper lobe of hDPP III is shown in yellow and the lower lobe of the protein is shown in gray. Interactions are pictured as yellow dashed lines.

4. 1. 2 hDPP III in complex with angiotensin-II

Angiotensin II (DRVYIHPF) is one of the main peptide players involved in the renin-angiotensin system, a physiological system that regulates blood pressure and fluid balance. The octapeptide angiotensin-II acts as a vasoconstrictor [1, 7]. DPP III has been shown to cleave the peptide in vitro, suggesting involvement of the protein in blood pressure regulation [1]. To determine binding parameters of hDPP III and angiotensin-II, ITC measurements were performed. A K_d of 1.64 µM was determined, indicating a strong binding. The binding process was shown to be endothermic and entropy driven, as observed by *Bezerra et al.* for tynorphin and hDPP III [3]. Cocrystallization of hDPP III in complex with the octapeptide angiotensin-II was conducted to show how the protein binds to longer peptides. The structure was determined by Prashant Kumar at a resolution of 2.40 Å [18].

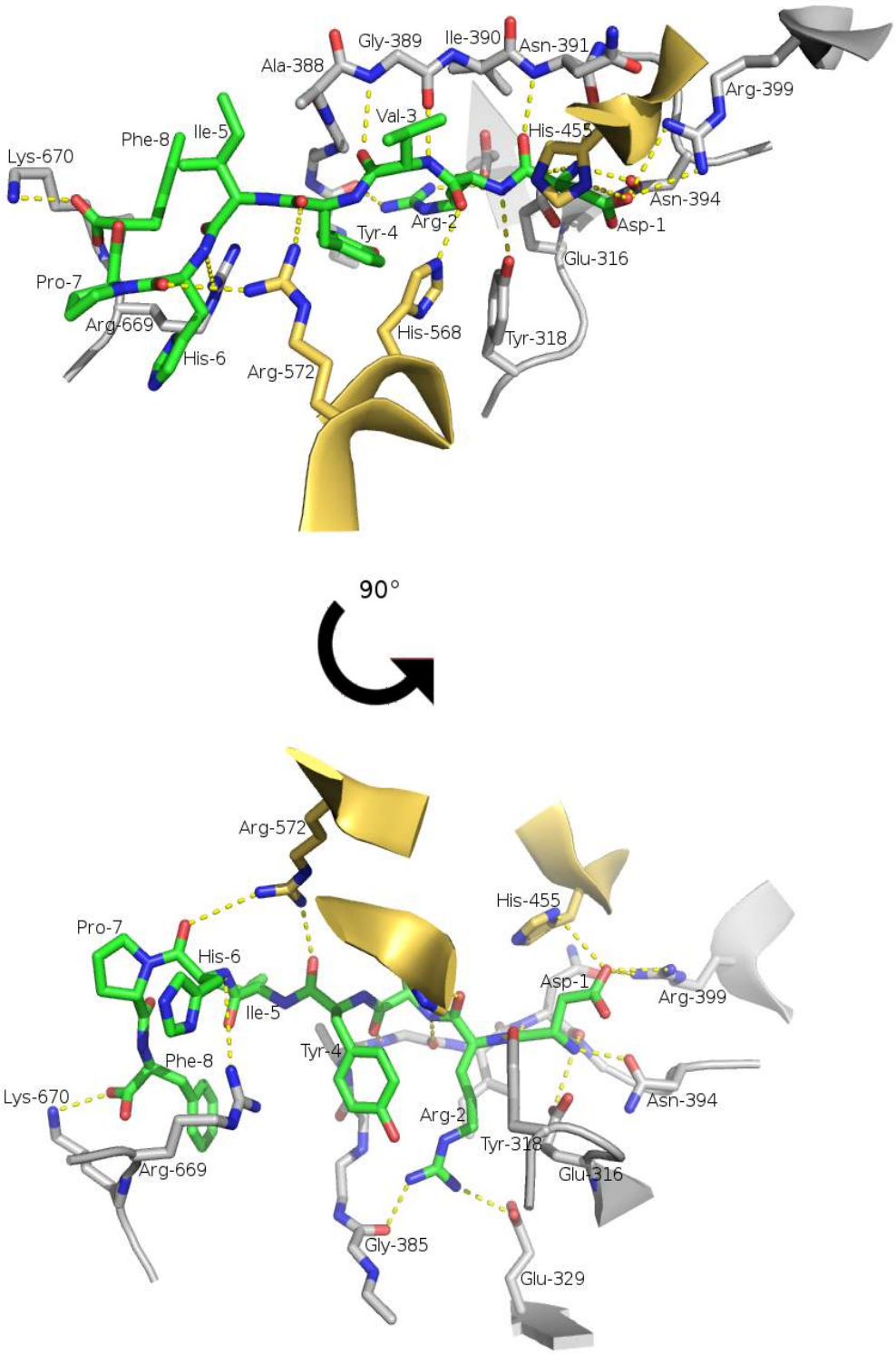

Figure 23: Interactions of hDPP III with angiotensin-II (adapted from [18], PDB: 5E2Q)

Angiotensin-II is shown in green, the upper lobe of hDPP III is shown in yellow and the lower lobe of the protein is colored gray. Interactions are shown as yellow dashed lines.

Figure 23 shows the residues of hDPP III involved in binding angiotensin-II. Most interactions are polar interactions contributed from the lower lobe of the protein. Three interactions are provided from the upper lobe of hDPP III, from the conserved His-568, from His-455, and from Arg-572. The N-terminal end of angiotensin-II forms an extended β-strand, which binds to the 5-stranded β-core of hDPP III in an antiparallel fashion. Ala-388 to Asn-391 are part of the β-core and interact with angiotensin-II via hydrogen bonds. Moreover, angiotensin-II is anchored in the binding cleft by Asn-394, Glu-316 and Tyr-318. The peptide has a turn at its C-terminal end, due to a cis-peptide formed between His-6 and Pro-7 [18]. This conformation has also been observed in structures of angiotensin-II in aqueous environment [22]. The C-terminus of angiotensin-II is stabilized by polar interactions provided from Arg-669 and Lys-670. The structure of hDPP III in complex with angiotensin-II does not contain the catalytic Zn-ion. The Zn-ion was most likely sequestered over time, because the crystallization condition used (Index #19, Hampton Research) contains phosphate, which is known to sequester divalent cations [18].

4. 1. 3 hDPP III in complex with leu-enkephalin

Leu-Enkephalin is another peptide involved in nociception that was shown to be hydrolyzed by DPP III in vitro [1]. The structure of hDPP III and leu-enkephalin was determined by Prashant Kumar at 2.05 Å resolution.

Interactions between hDPP III and leu-enkephalin are shown in figure 24. Leu-enkephalin and met-enkephalin bind to the protein in a similar fashion. The N-terminus of leu-enkephalin is anchored to the protein by hydrogen bonds provided from the 5-stranded β-core (Ala-388 to Asn-391) and from Glu-316, Tyr-318 and Asn-394. Moreover, His-568 interacts with the ligand. Another residue from the upper lobe, Arg-572, binds to the substrate via a hydrogen bond. This interaction could not be observed in the structure of hDPP III in complex with met-enkephalin. Arg-669, which is involved in binding met-enkephalin, does not interact with leu-enkephalin [18].

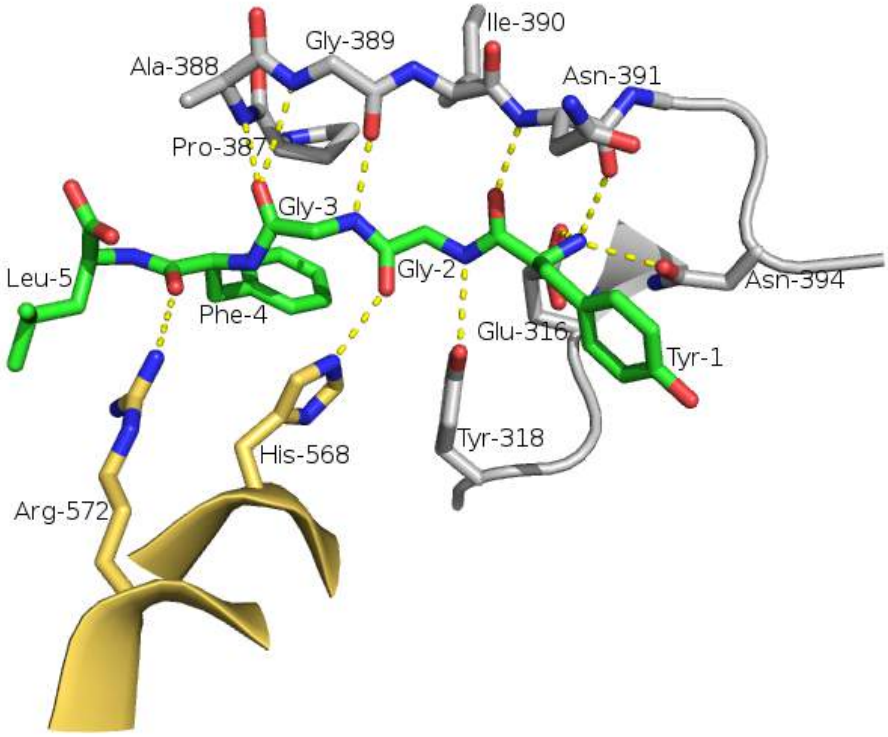

Figure 24: Interactions of hDPP III with leu-enkephalin (adapted from [18], PDB: 5E3A)

Leu-enkephalin is shown in green, the upper lobe of hDPP III is shown in yellow and the lower lobe of the protein is colored gray. Interactions are pictured as yellow dashed lines.

4. 1. 4 hDPP III in complex with IVYPW

Another structure, which was obtained in this project, is the structure of hDPP III in complex with IVYPW. Crystallization and structure determination were conducted by Manuel Reisinger [18]. Same as tynorphin (VVYPW), IVYPW is a hemorphin-like peptide. Both peptides were shown to inhibit hDPP III, IVYPW is suggested to inhibit the protein more effectively [6]. A crystal structure of hDPP III in complex with IVYPW was obtained at a resolution of 2.76 Å.

As shown in figure 25, IVYPW interacts with residues from the 5-stranded β-core (Ala-388 to Asn-391), as well as Asn-394 from the lower lobe of the

protein. Arg-669 forms a strong hydrogen bond to the C-terminal end of the peptide. Also, the conserved His-568 from the upper lobe of hDPP III interacts with IVYPW. Interestingly, IVYPW also interacts with the Zn-ion. This interaction was not observed in case of angiotensin-2, met-enkephalin and leu-enkephalin [18].

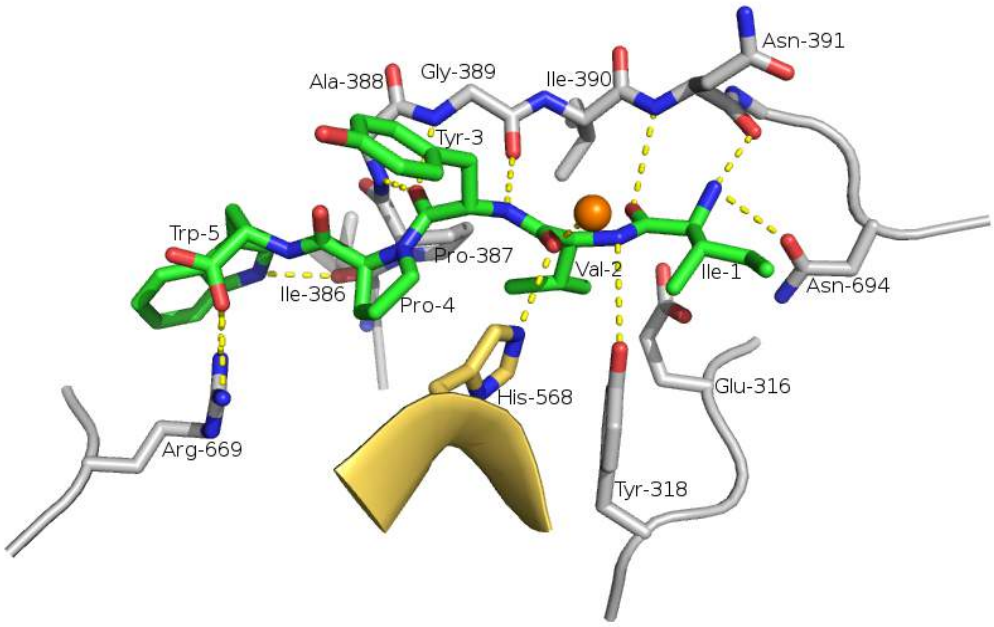

Figure 25: Interactions of hDPP III with IVYPW (adapted from [18], PDB: 5E3C)

IVYPW is shown in green, the upper lobe of hDPP III is colored yellow and the lower lobe of the protein is shown in gray. Interactions are pictured as yellow dashed lines. The Zn-ion is pictured as a orange sphere.

4.2 Binding modes and their influence on catalysis

Some ligands of hDPP III are hydrolyzed efficiently (for instance met-enkephalin, leu-enkephalin, angiotensin-II, endomorphin-2), whereas other ligands get cut very slowly. Tynorphin and IVYPW are cleaved by hDPP III, but this process is very slow and the peptides are therefore often referred to as a inhibitors of the enzyme [6, 14].

In the structures discussed in this thesis two different binding modes are observable. A comparison between the binding mode of hDPP III to met-enkephalin (as a representative of substrates that get hydrolyzed fast) and the binding mode of hDPP III to IVYPW (which is presumed to be an inhibitor of the enzyme) is shown in figure 26. Glu-451 shown in the picture is modeled, because an inactive variant of hDPP III was used for crystallization. In the structure of hDPP III in complex with met-enkephalin, a water molecule completes the tetrahedral coordination of the catalytic Zn-ion. When IVYPW is bound to hDPP III, the ligand is in contact with the Zn-ion and the water molecule is thereby displaced [18].

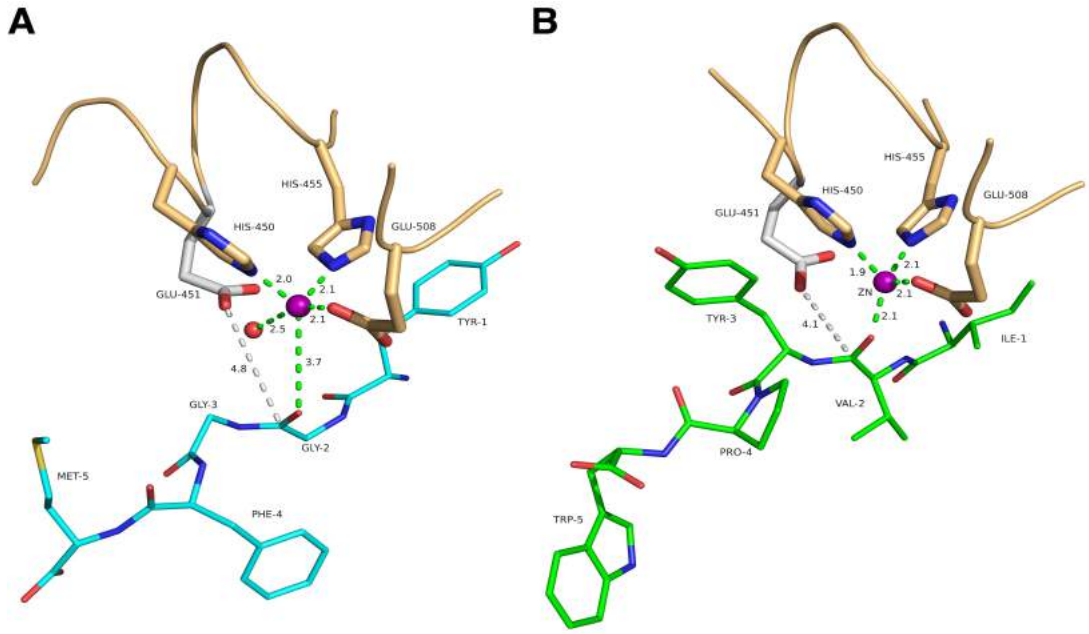

Figure 26: Comparison of binding modes (reused from [18])

The catalytic Zn-ion is shown as a magenta sphere, the water molecule is shown in red. Residues involved in coordination of the Zn-ion are labeled and shown in orange. Glu-451 was modeled based on the structure of open hDPP III [3], it is colored light gray. Potential interactions with the Zn-ion are shown as green dashed lines, the distance between the carboxylate carbon of Glu-451 and the carbon of the scissile peptide bond is shown as a grey dashed line. **A:** hDPP III in complex with met-enkephalin (cyan). A distance of 3.7 Å was measured between the catalytic Zn-ion and the carbonyl oxygen of the scissile peptide bond. **B:** hDPP III in complex with IVYPW (green). The carbonyl oxygen of the scissile peptide bond interacts with the Zn-ion and thereby displaces the water molecule.

Surprisingly, interaction of the ligand with the catalytic Zn-ion was also observed in the structure of hDPP III in complex with endomorphin-2, although endomorphin-2 is not an inhibitor or „slow" substrate of the enzyme. However, the electron density observed for the ligand in this structure was not well defined in central parts of the ligand and an occupancy below 100% is observable for endomorphin-2.

The observed difference in the binding mode may explain why met-enkephalin is hydrolyzed well by hDPP III, but IVYPW is not. The catalytic mechanism proposed by *Baral et al.* for yDPP III most likely also applies to hDPP III and is pictured in figure 27 A. This mechanism was suggested because of the similarity of the yDPP III active site to the active site of other metallopeptidases like thermolysin and neprilysin [2]. A similar mechanism was also found to be used for peptide hydrolysis by Carboxypeptidase A, where it is referred to as the „promoted-water pathway" [23].

According to the promoted-water mechanism, Glu-451 of hDPP III deprotonates the water molecule in contact with the Zn-ion. The water molecule thereby becomes a nucleophile and attacks the scissile peptide bond. This leads to the formation of a transition state (shown on the right in figure 27 A), in which the carbonyl oxygen completes the tetrahedral coordination of the Zn-ion. His-568 stabilizes the tetrahedral intermediate. The intermediate can be split via protonation of the leaving nitrogen group by Glu-451. The promoted-water mechanism can be applied on substrates like met-enkephalin, which do not directly interact with the catalytic Zn-ion.

When IVYPW is bound to hDPP III, the water molecule in the active site is displaced and the promoted-water pathway cannot take place. Another catalytic pathway may be chosen in this case [18]. The anhydride mechanism (shown in figure 27 B) is suggested as a catalytic mechanism for hDPP III because of the similar active site arrangements observed in hDPP III and Carboxypeptidase A. It is proposed to be used by Carboxypeptidase A to hydrolyze esters at a low temperature [23]. Adopted to hDPP III, peptide hydrolysis using the the anhydride mechanism starts with Glu-451 directly attacking the carbonyl carbon of the scissile peptide bond. Thereby an acyl-enzyme-like intermediate is formed. The pathway is energetically

unfavorable and therefore inefficient, but it may be applied to „slow" substrates like IVYPW [18].

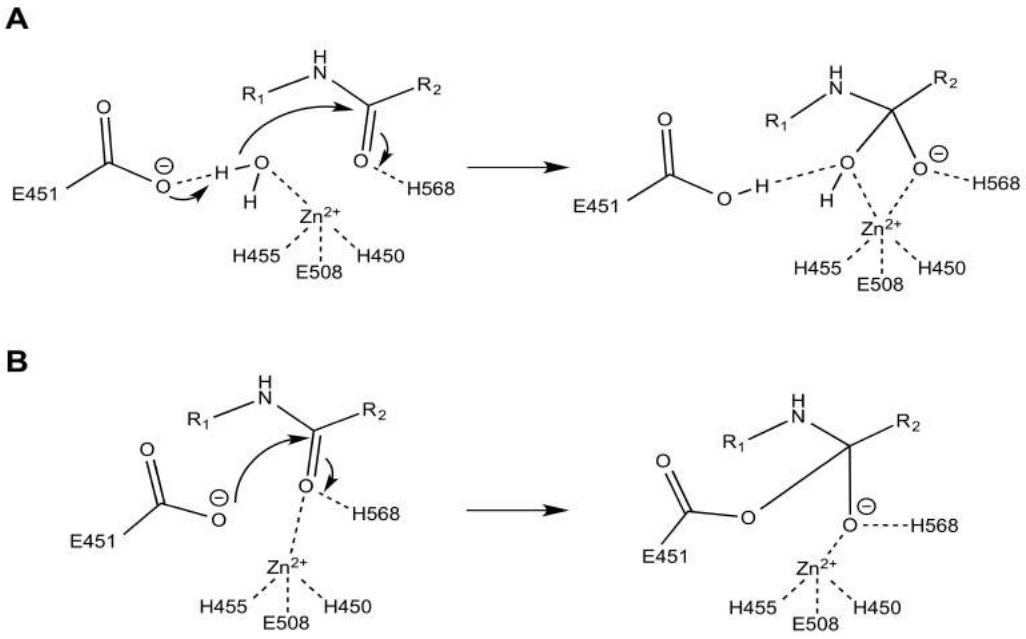

Figure 27: Proposed catalytic mechanisms for hDPP III (reused from [18])

A shows the promoted-water mechanism, **B** pictures the anhydride mechanism.

4.3 Anion-π interaction

Aromatic rings are involved in several types of noncovalent interactions that can be found in biological molecules. π-stacking, the interaction between two aromatic rings, is widely recognized and well known for its stabilizing effect in DNA. Cation-π interactions can be formed between a cation and an aromatic ring. They are known to play a role in formation of protein-ligand interactions and in protein structure [24]. Interactions between a negatively charged group and the positively charged potential at the ring edge of an aromatic group are called anion-π or anion-aromatic interactions [17, 24]. *Schwans et al.* suggested an anion-π interaction is used to put the general base in ketosteroid isomerase from *Comamonas testosteroni* in place. They also point out that Phe residues may occur frequently in this kind of interaction, because they are able to bind hydrophobic substrates simultaneously [17]. In hDPP III, an anion-π

interaction is suspected to have a similar function. Phe-373 may interact with Glu-451 in order to position Glu-451 in the active site of the protein. The suspected interaction in active unbound hDPP III (PDB: 3FVY) [3] is shown in figure 28.

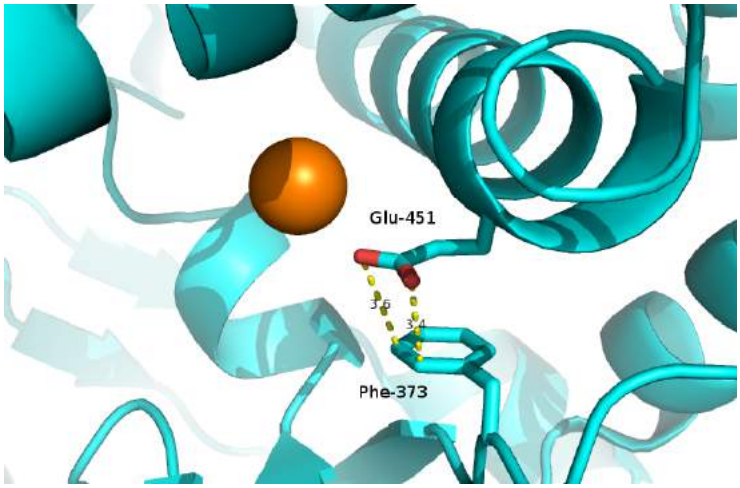

Figure 28: Anion-π interaction between Glu-451 and Phe-373

The suspected anion-π interaction between Glu-451 and Phe-373 is indicated by yellow dashed lines. The Zn-ion is shown as a orange sphere.

Fluorescent activity assays were carried out with wtDPP III and the active hDPP III F373L mutant to verify the interaction. A 20-fold reduction of catalytic activity was observed upon exchange of Phe-373 with Leu, the K_M remained unchanged. The reduction of activity confirms, that an interaction between Phe-373 and Glu-451 is present and that this interaction is important for catalytic activity of hDPP III.

An anion-π interaction between those residues is not only lost upon mutation of Phe-373, but also when the enzyme is rendered inactive by mutation of Glu-451. It is therefore possible, that the exchange of Glu-451 by Ala slightly alters the conformational properties of hDPP III.

4.4 Conclusions

When no ligand is bound hDPP III is an elongated protein with an upper and a lower lobe, divided by a large cleft that is proposed to be the ligand binding site. Upon binding of tynorphin, the lobes were shown to move towards each other as rigid bodies to bury the ligand in the binding site and the protein has an almost globular shape [3]. By determining structures of hDPP III in complex with met-enkephalin and endomorphin-2, it could be shown that this large conformational change also occurs when other ligands bind to the protein. Along with those structures, the structures of hDPP III in complex with angiotensin-II, leu-enkephalin and IVYPW were analyzed [18]. The ligands were found to bind to the enzyme in a similar way. Most ligands bind as a extended β-strand in an antiparallel fashion to the 5-stranded β-core of hDPP III, which was observed to be involved in ligand binding in all structures that were analyzed.

A significant difference was observed in the binding modes of substrates and „slow" substrates or inhibitors. Substrates, that are hydrolyzed well, do not interact with the Zn-ion. In contrast, inhibitors interact with the Zn-ion, thereby displacing the water molecule that is involved in hydrolysis. The energetically favorable promoted-water mechanism, which is usually used for substrate hydrolysis, is not applicable when the ligand is in contact with the Zn ion. The connection between Zn-ion contact and the sequence of the ligand still remains unclear [18].

An anion-π interaction between Phe-373 and Glu-451 was suspected to play an important role for substrate hydrolysis by putting Glu-451 in place. A 20-fold reduction of catalytic activity was observed when the interaction was annulled. This indicates that the suspected anion-π interaction indeed is important for catalytic activity of hDPP III.

5. List of figures

Figure 1: Open yDPP III and hDPP III.....10
Figure 2: hDPP III in complex with tynorphin.....11
Figure 3: Partial sequence alignment of mDPP III and shortened mDPP III....22
Figure 4: Partial sequence alignment of active hDPP III and hDPP III F373L..23
Figure 5: Affinity chromatography, Coomassie-stained gel.....24
Figure 6: Reverse affinity chromatography, Coomassie-stained gel.....25
Figure 7: Anion exchange chromatography, Coomassie-stained gel 1.....26
Figure 8: Anion exchange chromatography, Coomassie-stained gel 2.....26
Figure 9: Size exclusion chromatography, Coomassie-stained gel.....27
Figure 10: hDPP III crystals.....28
Figure 11: Overall structure of inactive hDPP III in complex with met-enkephalin.....30
Figure 12: Interactions of inactive hDPP III with met-enkephalin.....31
Figure 13: Electron density of met-enkephalin bound to hDPP III (reused from [18]).....32
Figure 14: Overall structure of inactive hDPP III in complex with endomorphin-2.....33
Figure 15: Interactions of inactive hDPP III with endomorphin-2.....33
Figure 16: Electron density of endomorphin-2 bound to hDPP III (reused from [18]).....34
Figure 17: Michaelis-Menten kinetics of wtDPP III and hDPP III F373L.....35
Figure 18: ITC of inactive hDPP III and angiotensin-II.....36
Figure 19: Intermolecular disulfide bridge (reused from [18]).....38
Figure 20: Superposition of ligand-bound hDPP III.....38
Figure 21: Superposition of ligands bound to inactive hDPP III (adapted from [18]).....39
Figure 22: Interactions of hDPP III with tynorphin (adapted from [3], PDB: 3T6B).....40
Figure 23: Interactions of hDPP III with angiotensin-II (adapted from [18], PDB: 5E2Q).....41
Figure 24: Interactions of hDPP III with leu-enkephalin (adapted from [18], PDB: 5E3A).....43

Figure 25: Interactions of hDPP III with IVYPW (adapted from [18], PDB: 5E3C).....44
Figure 26: Comparison of binding modes (reused from [18]).....45
Figure 27: Proposed catalytic mechanisms for hDPP III (reused from [18])...47
Figure 28: Anion-π interaction between Glu-451 and Phe-373.....48

6. List of tables

Table 1: Primers used for site-directed mutagenesis of mDPP III and hDPP III F373L.....14

Table 2: Thermocycler program used for site-directed mutagenesis.....15

Table 3: Buffers used for Zn-ion chelation.....17

Table 4: Crystallographic data and refinement statistics.....29

Table 5: Enzyme kinetics of wtDPP III and hDPP III F373L.....35

Table 6: Thermodynamic parameters of inactive hDPP III and angiotensin-II.36

7. References

1. Prajapati SC, Chauhan SS. Dipeptidyl peptidase III: a multifaceted oligopeptide N-end cutter. FEBS J. 2011 Sep;278(18):3256–76.

2. Baral PK, Jajcanin-Jozić N, Deller S, Macheroux P, Abramić M, Gruber K. The first structure of dipeptidyl-peptidase III provides insight into the catalytic mechanism and mode of substrate binding. J Biol Chem. 2008 Aug 8;283(32):22316–24.

3. Bezerra GA, Dobrovetsky E, Viertlmayr R, Dong A, Binter A, Abramic M, et al. Entropy-driven binding of opioid peptides induces a large domain motion in human dipeptidyl peptidase III. Proc Natl Acad Sci USA. 2012 Apr 24;109(17):6525–30.

4. Burkard TR, Planyavsky M, Kaupe I, Breitwieser FP, Bürckstümmer T, Bennett KL, et al. Initial characterization of the human central proteome. BMC Syst Biol. 2011;5:17.

5. Sato H, Kimura K, Yamamoto Y, Hazato T (2003) [Activity of DPP III in human cerebrospinal fluid derived from patients with pain]. Masui. The Japanese journal of anesthesiology 52 (3): 257–263.

6. Chiba T, Li Y-H, Yamane T, Ogikubo O, Fukuoka M, Arai R, et al. Inhibition of recombinant dipeptidyl peptidase III by synthetic hemorphin-like peptides. Peptides. 2003 May;24(5):773–8.

7. Viazzi F, Leoncini G, Pontremoli R. Antihypertensive treatment and renal protection: the role of drugs inhibiting the renin-angiotensin-aldosterone system. High Blood Press Cardiovasc Prev. 2013 Dec;20(4):273–82.

8. Barsun M, Jajcanin N, Vukelić B, Spoljarić J, Abramić M. Human dipeptidyl peptidase III acts as a post-proline-cleaving enzyme on endomorphins. Biol Chem. 2007 Mar;388(3):343–8.

9. Simaga S, Babić D, Osmak M, Ilić-Forko J, Vitale L, Milicić D, et al. Dipeptidyl peptidase III in malignant and non-malignant gynaecological tissue. Eur J Cancer. 1998 Feb;34(3):399–405.

10. Simaga S, Babić D, Osmak M, Sprem M, Abramić M. Tumor cytosol dipeptidyl peptidase III activity is increased with histological aggressiveness of ovarian primary carcinomas. Gynecol Oncol. 2003 Oct;91(1):194–200.

11. Liu Y, Kern JT, Walker JR, Johnson JA, Schultz PG, Luesch H. A genomic screen for activators of the antioxidant response element. Proc Natl Acad Sci USA. 2007 Mar 20;104(12):5205–10.

12. Zhan H, Yamamoto Y, Shumiya S, Kunimatsu M, Nishi K, Ohkubo I, et al. Peptidases play an important role in cataractogenesis: an immunohistochemical study on lenses derived from Shumiya cataract rats. Histochem J. 2001 Oct;33(9–10):511–21.

13. Fukasawa K, Fukasawa KM, Iwamoto H, Hirose J, Harada M. The HELLGH motif of rat liver dipeptidyl peptidase III is involved in zinc coordination and the catalytic activity of the enzyme. Biochemistry. 1999 Jun 29;38(26):8299–303.

14. Yamamoto Y, Hashimoto J, Shimamura M, Yamaguchi T, Hazato T. Characterization of tynorphin, a potent endogenous inhibitor of dipeptidyl peptidaseIII. Peptides. 2000 Apr;21(4):503–8.

15. Maurer R, Römer D, Büscher HH, Gähwiler BH, Thies PW, David S. Valorphin: a novel chemical structure with opioid activity. Neuropeptides. 1985 Feb;5(4–6):387–90.

16. Abramić M, Zubanović M, Vitale L. Dipeptidyl peptidase III from human erythrocytes. Biol Chem Hoppe-Seyler. 1988 Jan;369(1):29–38.

17. Schwans JP, Sunden F, Lassila JK, Gonzalez A, Tsai Y, Herschlag D. Use of anion-aromatic interactions to position the general base in the ketosteroid isomerase active site. Proc Natl Acad Sci USA. 2013 Jul 9;110(28):11308–13.

18. Kumar P, Reithofer V, Reisinger M, Wallner S, Pavkov-Keller T, Macheroux P, et al. Substrate complexes of human dipeptidyl peptidase III reveal the mechanism of enzyme inhibition. Scientific Reports. 2016 Mar 30;6:23787.

19. Hirose J, Iwamoto H, Nagao I, Enmyo K, Sugao H, Kanemitu N, et al. Characterization of the metal-substituted dipeptidyl peptidase III (rat liver). Biochemistry. 2001 Oct 2;40(39):11860–5.

20. Newman J. Novel buffer systems for macromolecular crystallization. Acta Crystallogr D Biol Crystallogr. 2004 Mar;60(Pt 3):610–2.

21. Jajčanin-Jozić N, Tomić S, Abramić M. Importance of the three basic residues in the vicinity of the zinc-binding motifs for the activity of the yeast dipeptidyl peptidase III. J Biochem. 2014 Jan;155(1):43–50.

22. Carpenter KA, Wilkes BC, Schiller PW. The octapeptide angiotensin II adopts a well-defined structure in a phospholipid environment. Eur J Biochem. 1998 Jan 15;251(1–2):448–53.

23. Xu D, Guo H. Quantum mechanical/molecular mechanical and density functional theory studies of a prototypical zinc peptidase (carboxypeptidase A) suggest a general acid-general base mechanism. J Am Chem Soc. 2009 Jul 22;131(28):9780–8.

24. Frontera A, Gamez P, Mascal M, Mooibroek TJ, Reedijk J. Putting anion-π interactions into perspective. Angew Chem Int Ed Engl. 2011 Oct 4;50(41):9564–83.

8. Appendix

Sequence alignment mDPP III

The sequence of mDPP III codon-optimized for expression in *E. coli* is labeled as „mouseDPP3". The sequencing result after shortening the gene was aligned to this sequence, it is labeled as „mouseDPP3-shortened". The nucleotides exchanged by site-directed mutagenesis are highlighted red. The primer used for sequencing is complementary to the T7 terminator sequence contained in the vector, therefore a part of the vector is included in the sequencing result (highlighted gray). Some artifacts can be observed in the sequencing result at the end of the read.

```
CLUSTAL O(1.2.1) multiple sequence alignment

mouseDPP3               ATGGCAGATACCCAGTATATTCTGCCGAATGATATTGGTGTTAGCAGCCTGGATTGTCGT   60
mouseDPP3-shortened     ------------------------------------------------------------   0

mouseDPP3               GAAGCATTTCGTCTGCTGAGCCCGACCGAACGTCTGTATGCACATCATCTGAGCCGTGCA   120
mouseDPP3-shortened     ------------------------------------------------------------   0

mouseDPP3               GCATGGTATGGTGGTCTGGCAGTTCTGCTGCAGACCAGTCCGGAAGCACCGTATATCTAT   180
mouseDPP3-shortened     ------------------------------------------------------------   0

mouseDPP3               GCACTGCTGAGTCGTCTGTTTCGTGCACAGGATCCAGATCAGCTGCGTCAGCATGCACTG   240
mouseDPP3-shortened     ------------------------------------------------------------   0

mouseDPP3               GCAGAAGGTCTGACCGAAGAAGAATATCAGGCATTTCTGGTTTATGCAGCCGGTGTTTAT   300
mouseDPP3-shortened     ------------------------------------------------------------   0

mouseDPP3               AGCAATATGGGCAACTATAAAAGCTTCGGCGATACCAAATTTGTTCCGAATCTGCCTAAA   360
mouseDPP3-shortened     ------------------------------------------------------------   0

mouseDPP3               GATAAACTGGGTCGTGTTATTCTGGGTAGCAAAGCAGCACAGCAGCGTCCGGAAGAGGTT   420
mouseDPP3-shortened     ------------------------------------------------------------   0

mouseDPP3               CGTGATCTGTGGCAGACCTGTGGTGATCTGATGTTTAGCCTGGAACCGCGTCTGCGTCAT   480
mouseDPP3-shortened     ------------------------------------------------------------   0

mouseDPP3               CTGGGTCTGGGTAAAGAAGGTGTTACCACCTATTTTAGCGGTGATTGTACCATGGAAGAT   540
mouseDPP3-shortened     ------------------------------------------------------------   0

mouseDPP3               GCAAAACTGGCACAGGATTTTCTGGATAGCCAGAATCTGAGCGCATATAATACCCGTCTG   600
mouseDPP3-shortened     ------------------------------------------------------------   0


mouseDPP3               TTTAAAGTTGTTGGTCAAGAGGGTAAAAGCCATTATGAAGTTCGTCTGGCAAGCGTTCTG   660
mouseDPP3-shortened     ------------------------------------------------------------   0

mouseDPP3               AATACCGATCCGGCACTGGATAGCGAACTGACCAGCAAACTGAAACGTTATGAATTTCAG   720
mouseDPP3-shortened     ------------------------------------------------------------   0

mouseDPP3               GGCAACCATTTTCAGGTTACCCGTGGTGATTATGCACCGATCCTGCAGAAAGTTGTGGAA   780
mouseDPP3-shortened     ------------------------------------------------------------   0
```

```
mouseDPP3               CATCTGGAAAAAGCAAAAGCCTATGCAGCAAATAGCCATCAAGAGCAGATGCTGGCACAG   840
mouseDPP3-shortened     ------------------------------------------------------------   0

mouseDPP3               TATGTTGAAAGTTTTACCCAGGGTAGCATTGAAGCACATAAACGTGGTAGCCGTTTTTGG   900
mouseDPP3-shortened     ------------------------------------------------------------   0

mouseDPP3               ATTCAGGATAAAGGTCCGATTGTGGAAAGCTATATTGGCTTTATTGAAAGCTATCGCGAT   960
mouseDPP3-shortened     ------------------------------------------------------------   0

mouseDPP3               CCGTTTGGTAGTCGTGGTGAATTTGAAGGTTTTGTTGCCATGGTGAATAAAGCAATGAGC   1020
mouseDPP3-shortened     ------------------------------------------------------------   0

mouseDPP3               GCCAAATTTGAACGTCTGGTTGCAAGCGCAGAACAGCTGCTGAAAGAACTGCCGTGGCCT   1080
mouseDPP3-shortened     ------------------------------------------------------------   0

mouseDPP3               CTGGCATTTGAAAAAGATAAATTTCTGACACCGGATTTCACCAGTCTGGATGTTCTGACC   1140
mouseDPP3-shortened     ------------------------------------------------------------C  1
                                                                                     *

mouseDPP3               TTTGCAGGTAGCGGTATTCC-GGCAGGTA-TTAACATTCCGAATTATGATGATCTGCGTC   1198
mouseDPP3-shortened     TTTGCAGGTAGCGGTATTCCCGGCAGGTATTAACATTCCGAAATTATGATGATCTGCGTC   61
                        ******************* ******** * *   * *  ******************

mouseDPP3               AGACCGAAGGCTTTAAAAACGTTAGCCTGGGTAATGTTCTGGCCGTTGCGTATGCAGCCA   1258
mouseDPP3-shortened     AGACCGAAGGCTTTAAAAACGTTAGCCTGGGTAATGTTCTGGCCGTTGCGTATGCAGCCA   121
                        ************************************************************

mouseDPP3               AACGTGAAAAACTGACCTTTCTGGAAGAAGAGGATAAAGATCTGTATATCCGTTGGAAAG   1318
mouseDPP3-shortened     AACGTGAAAAACTGACCTTTCTGGAAGAAGAGGATAAAGATCTGTATATCCGTTGGAAAG   181
                        ************************************************************

mouseDPP3               GTCCGTCATTTGATGTTCAGGTTGGTCTGCATGAACTGCTGGGTCATGGTAGTGGTAAAC   1378
mouseDPP3-shortened     GTCCGTCATTTGATGTTCAGGTTGGTCTGCATGAACTGCTGGGTCATGGTAGTGGTAAAC   241
                        ************************************************************

mouseDPP3               TGTTTGTTCAGGATGAAAAAGGTGCCTTTAACTTTGACAAAGAAACCGTGATTAATCCGG   1438
mouseDPP3-shortened     TGTTTGTTCAGGATGAAAAAGGTGCCTTTAACTTTGACAAAGAAACCGTGATTAATCCGG   301
                        ************************************************************

mouseDPP3               AAACCGGTGAGCAGATTCAGAGCTGGTATCGTAGCGGTGAAACCTGGGATAGCAAATTTA   1498
mouseDPP3-shortened     AAACCGGTGAGCAGATTCAGAGCTGGTATCGTAGCGGTGAAACCTGGGATAGCAAATTTA   361
                        ************************************************************

mouseDPP3               GCACCATTGCAAGCAGCTATGAAGAATGTCGTGCAGAAAGCGTTGGTCTGTATCTGTGTC   1558
mouseDPP3-shortened     GCACCATTGCAAGCAGCTATGAAGAATGTCGTGCAGAAAGCGTTGGTCTGTATCTGTGTC   421
                        ************************************************************

mouseDPP3               TGAATCCGCAGGTTCTGGAAATTTTTGGTTTTGAAGGTGCAGATGCCGAGGATGTGATTT   1618
mouseDPP3-shortened     TGAATCCGCAGGTTCTGGAAATTTTTGGTTTTGAAGGTGCAGATGCCGAGGATGTGATTT   481
                        ************************************************************
mouseDPP3               ATGTTAATTGGCTGAATATGGTTCGTGCAGGTCTGCTGGCACTGGAATTCTATACACCGG   1678
mouseDPP3-shortened     ATGTTAATTGGCTGAATATGGTTCGTGCAGGTCTGCTGGCACTGGAATTCTATACACCGG   541
                        ************************************************************

mouseDPP3               AAGCAGCAAATTGGCGTCAGGCACACATGCAGGCACGTTTTGTGATTCTGCGTGTTCTGC   1738
mouseDPP3-shortened     AAGCAGCAAATTGGCGTCAGGCACACATGCAGGCACGTTTTGTGATTCTGCGTGTTCTGC   601
                        ************************************************************

mouseDPP3               TGGAAGCCGGTGAAGGTCTGGTTACCGTTACCCCGACCACCGGTAGTGATGGTCGTCCGG   1798
mouseDPP3-shortened     TGGAAGCCGGTGAAGGTCTGGTTACCGTTACCCCGACCACCGGTAGTGATGGTCGTCCGG   661
                        ************************************************************

mouseDPP3               ATGCACGTGTGCGTCTGGATCGTAGCAAAATTCGTAGCGTTGGCCGTCCTGCACTGGAAC   1858
mouseDPP3-shortened     ATGCACGTGTGCGTCTGGATCGTAGCAAAATTCGTAGCGTTGGCCGTCCTGCACTGGAAC   721
                        ************************************************************

mouseDPP3               GTTTTCTGCGTCGTCTGCAGGTACTGAAAAGCACCGGTGATGTTGTTGCAGGTCGTGCAC   1918
mouseDPP3-shortened     GTTTTCTGCGTCGTCTGCAGGTACTGAAAAGCACCGGTGATGTTGTTGCAGGTCGTGCAC   781
                        ************************************************************

mouseDPP3               TGTATGAAGGTTATGCAGCAGTTACCGATGCACCGCCTGAATGTTTTCTGACCCTGCGTG   1978
mouseDPP3-shortened     TGTATGAAGGTTATGCAGCAGTTACCGATGCACCGCCTGAATGTTTTCTGACCCTGCGTG   841
                        ************************************************************

mouseDPP3               ATACCGTGCTGCTGCGTAAAGAAAGCCGTAAACTGATTGTGCAGCCGAATACACGTCTGG   2038
mouseDPP3-shortened     ATACCGTGCTGCTGCGTAAAGAAAGCCGTAAACTGATTGTGCAGCCGAATACACGTCTGG   901
                        ************************************************************

mouseDPP3               AAGGTAGCGAAGTTCAGCTGGTTGAATATGAAGCCAGCGCAGCAGGTCTGATTCGTAGCT   2098
mouseDPP3-shortened     AAGGTAGCGAAGTTCAGCTGGTTGAATATGAAGCCAGCGCAGCAGGTCTGATTCGTAGCT   961
                        ************************************************************
```

```
mouseDPP3               TTTGTGAACGCTTTCCGGAAGATGGTCCGGAACTGGAAGAGGTGCTGATTCAGCTGGCAG   2158
mouseDPP3-shortened     TTTGTGAACGCTTTCCGGAAGATGGTCCGGAACTGGAAGAGGTGCTGATTCAGCTGGCAG   1021
                        ************************************************************

mouseDPP3               CAGCAGATGCACGTTTTTGGCGTAATCAGGCACAAGAAGCACCTCCGGGTCAGGCA----   2214
mouseDPP3-shortened     CAGCAGATGCACGTTTTTGGTAAAATCAGGCACAAGAAGCACCTCCGGGTCAGGCATAAC   1081
                        ******************   *********************************

mouseDPP3               ---------------------------------------------   2214
mouseDPP3-shortened     TCGAGCACCACCACCACCACCACTGAGATCCGGCTGCTAACAAA   1125
```

Sequence alignment hDPP III F373L

The sequence of active hDPP III (codon-optimized for expression in *E. coli*, containing mutations originally introduced for smFRET experiments) is labeled as „N6“. The mutated sequenced is labeled as „F373L – sequencing-result“. The nucleotide, that was exchanged by site-directed mutagenesis, is highlighted red. A mutation can be observed at the end of the read, it was interpreted as an sequencing artifact.

```
CLUSTAL O(1.2.1) multiple sequence alignment

N6                          ATGGCTGATACCCAGTACATTCTGCCTAACGATATTGGTGTTAGCTCCCTGGATTCCCGC       60
F373L-sequencing-result     ------------------------------------------------------------       0

N6                          GAAGCTTTCCGCCTGCTGTCCCCGACTGAGCGTCTGTACGCGTATCACCTGAGCCGCGCT       120
F373L-sequencing-result     ------------------------------------------------------------       0

N6                          GCCTGGTACGGTGGTCTGGCCGTGCTGCTGCAGACGTCTCCGGAGGCGCCTTACATCTAT       180
F373L-sequencing-result     ------------------------------------------------------------       0

N6                          GCGCTGCTGTCTCGTCTGTTCCGCGCGCAAGACCCGGACCAGCTGCGTCAGCACGCCCTG       240
F373L-sequencing-result     ------------------------------------------------------------       0

N6                          GCGGAGGGCCTGACCGAAGAAGAGTACCAAGCTTTCCTGGTTTACGCTGCGGGCGTCTAC       300
F373L-sequencing-result     ------------------------------------------------------------       0

N6                          TCCAACATGGGTAACTATAAAAGCTTCGGCGACACCAAATTTGTTCCGAACCTGCCGAAA       360
F373L-sequencing-result     ------------------------------------------------------------       0

N6                          GAGAAACTGGAGCGTGTAATCCTGGGCTCTGAGGCAGCTCAACAGCATCCGGAAGAGGTT       420
F373L-sequencing-result     ------------------------------------------------------------       0

N6                          CGTGGCCTGTGGCAGACCTGCGGCGAACTGATGTTCTCTCTGGAACCGCGTCTGCGTCAT       480
F373L-sequencing-result     ------------------------------------------------------------       0

N6                          CTGGGTCTGGGTAAAGAGGGCATCACCACTTACTTCTCCGGCAACTGTACTATGGAGGAC       540
F373L-sequencing-result     ------------------------------------------------------------       0

N6                          GCTAAACTGGCTCAGGACTTCCTGGATTCCCAGAATCTGTCCGCGTATAACACCCGCCTG       600
F373L-sequencing-result     ------------------------------------------------------------       0

N6                          TTCAAAGAAGTTGACGGCTGCGGTAAACCGTATTATGAAGTACGTCTGGCAAGCGTACTG       660
F373L-sequencing-result     ------------------------------------------------------------       0

N6                          GGTAGCGAACCTTCTCTGGATTCTGAGGTTACCTCCAAACTGAAAAGCTACGAATTCCGT       720
F373L-sequencing-result     ------------------------------------------------------------       0

N6                          GGCTCCCCATTTCAAGTAACCCGTGGCGACTACGCGCCGATCCTGCAGAAAGTAGTCGAG       780
F373L-sequencing-result     ------------------------------------------------------------       0

N6                          CAGCTGGAAAAAGCCAAAGCGTACGCCGCGAACTCTCACCAGGGCCAGATGCTGGCACAG       840
F373L-sequencing-result     ----------------------------------------AGGGCCAGATGCTGGCACAG       20
                                                                      ********************

N6                          TACATCGAGTCTTTCACTCAGGGTAGCATTGAGGCACACAAACGTGGTTCCCGTTTTTGG       900
F373L-sequencing-result     TACATCGAGTCTTTCACTCAGGGTAGCATTGAGGCACACAAACGTGGTTCCCGTTTTTGG       80
                            ************************************************************

N6                          ATCCAGGATAAAGGCCCTATCGTCGAGTCTTACATTGGTTTCATCGAATCTTACCGTGAT       960
F373L-sequencing-result     ATCCAGGATAAAGGCCCTATCGTCGAGTCTTACATTGGTTTCATCGAATCTTACCGTGAT       140
                            ************************************************************
```

```
N6                          CCTTTCGGTTCCCGCGGTGAGTTCGAAGGCTTCGTTGCTGTTGTGAACAAGGCTATGTCC       1020
F373L-sequencing-result     CCTTTCGGTTCCCGCGGTGAGTTCGAAGGCTTCGTTGCTGTTGTGAACAAGGCTATGTCC       200
                            ************************************************************

N6                          GCAAAATTTGAACGTCTGGTTGCCAGCGCTGAACAGCTGCTGAAGGAGCTGCCGTGGCCG       1080
F373L-sequencing-result     GCAAAATTTGAACGTCTGGTTGCCAGCGCTGAACAGCTGCTGAAGGAGCTGCCGTGGCCG       260
                            ************************************************************

N6                          CCGACCTTCGAGAAAGATAAATTCCTGACTCCGGACTTCACTAGCCTGGACGTTCTGACC       1140
F373L-sequencing-result     CCGACCTTCGAGAAAGATAAATTCCTGACTCCGGACCTCACTAGCCTGGACGTTCTGACC       320
                            ********************************** ***********************

N6                          TTCGCCGGCTCTGGCATTCCAGCTGGTATTAACATCCCGAATTATGACGACCTGCGCCAG       1200
F373L-sequencing-result     TTCGCCGGCTCTGGCATTCCAGCTGGTATTAACATCCCGAATTATGACGACCTGCGCCAG       380
                            ************************************************************

N6                          ACCGAAGGTTTCAAAAATGTGTCTCTGGGTAACGTACTGGCGGTCGCTTACGCGACTCAG       1260
F373L-sequencing-result     ACCGAAGGTTTCAAAAATGTGTCTCTGGGTAACGTACTGGCGGTCGCTTACGCGACTCAG       440
                            ************************************************************

N6                          CGTGAGAAACTGACCTTCCTGGAGGAGGATGACAAAGATCTGTATATCCTGTGGAAAGGT       1320
F373L-sequencing-result     CGTGAGAAACTGACCTTCCTGGAGGAGGATGACAAAGATCTGTATATCCTGTGGAAAGGT       500
                            ************************************************************

N6                          CCGTCCTTCGACGTCCAGGTCGGCCTGCACGAGCTGCTGGGTCACGGCTCCGGCAAACTG       1380
F373L-sequencing-result     CCGTCCTTCGACGTCCAGGTCGGCCTGCACGAGCTGCTGGGTCACGGCTCCGGCAAACTG       560
                            ************************************************************

N6                          TTCGTGCAGGACGAGAAAGGTGCTTTCAATTTCGACCAGGAAACCGTGATTAACCCGGAG       1440
F373L-sequencing-result     TTCGTGCAGGACGAGAAAGGTGCTTTCAATTTCGACCAGGAAACCGTGATTAACCCGGAG       620
                            ************************************************************

N6                          ACTGGTGAACAAATCCAGTCTTGGTATCGTTGCGGCGAAACCTGGGACAGCAAGTTCTCT       1500
F373L-sequencing-result     ACTGGTGAACAAATCCAGTCTTGGTATCGTTGCGGCGAAACCTGGGACAGCAAGTTCTCT       680
                            ************************************************************

N6                          ACTATCGCGAGCTCCTACGAGGAATGTCGTGCAGAGTCTGTTGGTCTGTATCTGAGCCTG       1560
F373L-sequencing-result     ACTATCGCGAGCTCCTACGAGGAATGTCGTGCAGAGTCTGTTGGTCTGTATCTGAGCCTG       740
                            ************************************************************

N6                          CACCCGCAGGTTCTGGAAATCTTCGGTTTCGAGGGCGCTGACGCCGAGGATGTGATCTAC       1620
F373L-sequencing-result     CACCCGCAGGTTCTGGAAATCTTCGGTTTCGAGGGCGCTGACGCCGAGGATGTGATCTAC       800
                            ************************************************************

N6                          GTTAACTGGCTGAACATGGTTCGTGCTGGTCTGCTGGCGCTGGAGTTTTACACCCCGGAG       1680
F373L-sequencing-result     GTTAACTGGCTGAACATGGTTCGTGCTGGTCTGCTGGCACTGG----------------       843
                            ************************************ ****
N6                          GCATTCAACTGGCGCCAAGCCCACATGCAGGCCCGTTTCGTAATCCTGCGTGTGCTGCTG       1740
F373L-sequencing-result     ------------------------------------------------------------       843

N6                          GAGGCTGGCGAAGGCCTGGTTACTATCACTCCGACCACGGGCTCTGATGGTCGTCCGGAT       1800
F373L-sequencing-result     ------------------------------------------------------------       843

N6                          GCGCGTGTCCGTCTGGACCGCTCTAAAATTCGTTCCGTAGGTAAACCAGCACTGGAGCGC       1860
F373L-sequencing-result     ------------------------------------------------------------       843

N6                          TTCCTGCGTCGTCTGCAGGTGCTGAAGAGCACTGGTGACGTTGCGGGCGGTCGTGCGCTG       1920
F373L-sequencing-result     ------------------------------------------------------------       843

N6                          TACGAGGGCTATGCTACCGTTACCGATGCACCGCCGGAGAGCTTCCTGACCCTGCGTGAC       1980
F373L-sequencing-result     ------------------------------------------------------------       843

N6                          ACTGTTCTGCTGCGTAAAGAATCTCGTAAGCTGATTGTTCAGCCGAATACCCGTCTGGAA       2040
F373L-sequencing-result     ------------------------------------------------------------       843

N6                          GGTTCTGACGTTCAGCTGCTGGAATATGAAGCATCCGCGGCCGGTCTGATCCGTAGCTTC       2100
F373L-sequencing-result     ------------------------------------------------------------       843

N6                          TCTGAGCGTTTCCCGGAAGATGGCCCGGAACTGGAAGAGATCCTGACCCAGCTGGCCACC       2160
F373L-sequencing-result     ------------------------------------------------------------       843

N6                          GCTGACGCGCGCTTTTGGAAGGGTCCGTCTGAGGCTCCTTCTGGCCAGGCCCTCGAGCGG       2220
F373L-sequencing-result     ------------------------------------------------------------       843

N6                          CACCACCACCACCACCACTGA      2241
F373L-sequencing-result     --------------------      843
```

Permission to reuse figures from: Kumar P, Reithofer V, Reisinger M, Wallner S, Pavkov-Keller T, Macheroux P, et al. Substrate complexes of human dipeptidyl peptidase III reveal the mechanism of enzyme inhibition. Scientific Reports. 2016 Mar 30;6:23787.

Dear Viktoria,

Thank you for contacting Nature Publishing Group. As an author, you have the right to use this manuscript and figures, as per the licence-to-publish you signed:
Ownership of copyright in the article remains with the Authors, and provided that, when reproducing the Contribution or extracts from it, the Authors acknowledge first and reference publication in the Journal, the Authors retain the following non-exclusive rights:

a) To reproduce the Contribution in whole or in part in any printed volume (book or thesis) of which they are the author(s).
b) They and any academic institution where they work at the time may reproduce the Contribution for the purpose of course teaching.
c) To post a copy of the Contribution as accepted for publication after peer review (in Word or Tex format) on the Authors' own web site or institutional repository, or the Authors' funding body's designated archive, six months after publication of the printed or online edition of the Journal, provided that they also give a hyperlink from the Contribution to the Journals web site.
d) To reuse figures or tables created by them and contained in the Contribution in other works created by them.

The above use of the term 'Contribution' refers to the author's own version, not the final version as published in the Journal.

Kind regards

Melissa Rose
Permissions Assistant

SpringerNature
The Macmillan Building
4 Crinan Street
London N1 9XW